

Department of Biotechnology and Chemical Technology

Noble Metal Catalysts in the Production of Biofuels

Andrea Gutiérrez



DOCTORAL
DISSERTATIONS

Noble Metal Catalysts in the Production of Biofuels

Andrea Gutiérrez

Doctoral dissertation for the degree of Doctor of Science in Technology to be presented with due permission of the School of Chemical Technology for public examination and debate in Auditorium KE2 (Komppa Auditorium) at the Aalto University School of Chemical Technology (Espoo, Finland) on the 18th of October, 2013, at 12 noon.

Aalto University
School of Chemical Technology
Department of Biotechnology and Chemical Technology
Industrial Chemistry

Supervising professor

Prof. A.O.I. Krause

Thesis advisor

Dr. M.L. Honkela

Preliminary examiners

Prof. K. Seshan

University of Twente, The Netherlands

Prof. R. Alén

University of Jyväskylä, Finland

Opponents

Dr. A. Lappas

Deputy Director Chemical Process Engineering Research Institute,
Center for Research and Technology Hellas, Greece

Aalto University publication series

DOCTORAL DISSERTATIONS 140/2013

© Andrea Gutiérrez

ISBN 978-952-60-5322-6 (printed)

ISBN 978-952-60-5323-3 (pdf)

ISSN-L 1799-4934

ISSN 1799-4934 (printed)

ISSN 1799-4942 (pdf)

<http://urn.fi/URN:ISBN:978-952-60-5323-3>

Unigrafia Oy

Helsinki 2013

Finland

Author

Andrea Gutiérrez

Name of the doctoral dissertation

Noble Metal Catalysts in the
Production of Biofuels

Publisher School of Chemical Technology

Unit Department of Biotechnology and Chemical Technology

Series Aalto University publication series DOCTORAL DISSERTATIONS 140/2013

Field of research Industrial Chemistry

Manuscript submitted 6 May 2013

Date of the defence 18 October 2013

Permission to publish granted (date) 20 August 2013

Language English

Monograph

Article dissertation (summary + original articles)

Abstract

The energy demand is increasing in the world together with the need to ensure energy security and the desire to decrease greenhouse gas emissions. While several renewable alternatives are available for the production of electricity, e.g. solar energy, wind power, and hydrogen, biomass is the only renewable source that can meet the demand for carbon-based liquid fuels and chemicals. The technology applied in the conversion of biomass depends on the type and complexity of the biomass, and the desired fuel. Hydrogen and hydrogen-rich mixtures (synthesis gas) are promising energy sources as they are more efficient and cleaner than existing fuels, especially when they are used in fuel cells.

Hydrotreatment is a catalytic process that can be used in the conversion of biomass or biomass-derived liquids into fuels. In autothermal reforming (ATR), catalysts are used in the production of hydrogen-rich mixtures from conventional fuels or bio-fuels. The different nature of biomass and biomass-derived liquids and mineral oil makes the use of catalysts developed for the petroleum industry challenging. This requires the improvement of available catalysts and the development of new ones.

To overcome the limitations of conventional hydrotreatment and ATR catalysts, zirconia-supported mono- and bimetallic rhodium, palladium, and platinum catalysts were developed and tested in the upgrading of model compounds for wood-based pyrolysis oil and in the production of hydrogen, using model compounds for gasoline and diesel. Catalysts were also tested in the ATR of ethanol. For comparative purposes commercial catalysts were tested and the results obtained with model compounds were compared with those obtained with real feedstocks (hydrotreatment tests with wood-based pyrolysis oil and ATR tests with NExBTL renewable diesel).

Noble metal catalysts were active and selective in the hydrotreatment of guaiacol used as the model compound for the lignin fraction of wood-based pyrolysis oil and wood-based pyrolysis oil, and in the ATR of simulated gasoline and diesel, low sulfur diesel and ethanol for the production of hydrogen-rich mixture for fuel cells. In hydrotreatment and ATR, rhodium-containing catalysts were the most active, selective, and stable.

Keywords biofuels, wood-based biofuels, noble metal catalysts, pyrolysis oil, hydrotreatment, autothermal reforming, ethanol reforming

ISBN (printed) 978-952-60-5322-6

ISBN (pdf) 978-952-60-5323-3

ISSN-L 1799-4934

ISSN (printed) 1799-4934

ISSN (pdf) 1799-4942

Location of publisher Helsinki

Location of printing Helsinki

Year 2013

Pages 129

urn <http://urn.fi/URN:ISBN:978-952-60-5323-3>

PREFACE

The experimental work reported in this thesis was carried out at the Industrial Chemistry Group of Aalto University (formerly Helsinki University of Technology) between January 2006 and January 2011. The work was part of the projects FINSOFC (2002-2006) and SofcPower (2007-2011) financed by Tekes (The Finnish Funding Agency for Technology and Innovation) and BIOCOUP (2006-2011) financed by the European Union.

I am most grateful to my supervisor, Professor Outi Krause, for her support, advice and interest in my work. I thank the members of the projects especially Dr. Yrjö Solantausta, Dr. Anja Oasmaa and their research group from VTT Technical Research Center of Finland (VTT). Thanks also to Prof. Heeres and his group from the University of Groningen, the Netherlands for the valuable scientific discussions and excellent co-operation throughout the years.

I am indebted to the unconditional help and friendship offered by my instructor, Dr. Maija Honkela who inspired and encouraged me to finish this work. I am most grateful to Dr. Reetta Kaila for her scientific contributions and, most important, for her friendship. Warm thanks to all my co-authors, especially Dr. Reetta Karinen, and Dr. Sanna Airaksinen from the Industrial Chemistry Group, Aalto University, and Ms. Agnes Ardiyanti from the University of Groningen, for their help in the research. I want to thank Dr. Juha Linnekoski for all the help with the setups and analytical equipment and to Ms. Kati Vilonen for reading this work and helping me to make it more understandable.

I would like to thank all my colleagues at the Industrial Chemistry Group for providing a wonderful working atmosphere, and Dr. Tuula-Riitta Viljava and Ms. Arja Tuohino-Chance for their support throughout the years at the lab.

My gratitude and love to my friends for their support and encouragement. Finally, to my family that has been closer than ever during these years.

Lappeenranta, 9th August 2013

Andrea Gutiérrez

CONTENTS

LIST OF PUBLICATIONS.....	8
CONTRIBUTIONS.....	9
Abbreviations and symbols.....	10
1 Introduction.....	12
1.1 The European Union and the environment.....	13
1.2 Energy sources in Finland.....	14
1.3 Wood as raw material for fuels.....	15
2 Conversion of wood to fuels.....	16
2.1 Fermentation process.....	17
2.2 Thermal processes.....	18
2.3 Wood-based pyrolysis oils.....	19
2.3.1 Upgrading.....	19
2.3.2 Hydrotreatment.....	21
2.3.3 Hydrotreatment catalysts.....	22
2.3.4 Guaiacol as model compound.....	23
2.4 Side streams from pulping process to fuels.....	25
2.4.1 Crude tall oil.....	25
2.4.2 Crude sulfate turpentine.....	26
3 Production of bio-based synthesis gas.....	27
3.1 Main reactions of hydrocarbons.....	27
3.2 Commercial catalysts.....	30
4 Noble metal catalysts.....	31
5 Scope of the research.....	33
6 Materials and methods.....	34
6.1 Catalyst preparation, pretreatment, and characterization.....	35
6.2 Catalyst testing.....	37
6.2.1 Hydrotreatment of guaiacol.....	37
6.2.2 Hydrotreatment of wood-based pyrolysis oils.....	38
6.2.3 Autothermal reforming of simulated and conventional fuels.....	41
7 Hydrotreatment.....	44

7.1	Guaiacol as model compound.....	44
7.1.1	Thermodynamics.....	44
7.1.2	Effect of temperature on the reactivity of guaiacol.....	45
7.1.3	Carbon deposition.....	48
7.2	Wood-based pyrolysis oil.....	49
7.2.1	Catalyst screening.....	50
7.2.2	Catalyst stability.....	53
8	Autothermal reforming.....	56
8.1	Simulated gasoline and diesel.....	56
8.1.1	Catalyst screening.....	57
8.1.2	Catalyst stability.....	59
8.2	Ethanol.....	59
8.2.1	Catalyst screening.....	60
8.2.2	Effect of reforming temperature.....	61
8.2.3	Stability of noble metal catalysts.....	62
8.3	Sulfur tolerance and autothermal reforming of commercial diesel.....	64
9	Concluding remarks.....	66
10	References.....	69

LIST OF PUBLICATIONS

This thesis consists of an overview and the following appended publications, which are referred to in the text by their Roman numeral.

- I A. Gutierrez, R.K. Kaila, M.L. Honkela, R. Slioor, A.O.I. Krause, Hydrodeoxygenation of guaiacol on noble metal catalysts, *Catalysis Today* 147 (2009) 239-246.
- II A.R. Ardiyanti, A. Gutierrez, M.L. Honkela, A.O.I. Krause, H.J. Heeres, Hydrotreatment of wood-based pyrolysis oil using zirconia-supported mono- and bimetallic (Pt, Pd, Rh) catalysts, *Applied Catalysis A: General* 407 (2011) 56-66.
- III R.K. Kaila, A. Gutiérrez, R. Slioor, M. Kemell, M. Leskelä, A.O.I. Krause, Zirconia-supported bimetallic RhPt catalysts: Characterization and testing in autothermal reforming of simulated gasoline, *Applied Catalysis B: Environmental* 84 (2008) 223-232.
- IV R.K. Kaila, A. Gutiérrez, A.O.I. Krause, Autothermal reforming of simulated and commercial diesel: The performance of zirconia-supported RhPt catalyst in the presence of sulfur, *Applied Catalysis B: Environmental* 84 (2008) 324-331.
- V R.K. Kaila, A. Gutiérrez, S.T. Korhonen, A.O.I. Krause, Autothermal reforming of *n*-dodecane, toluene, and their mixture on mono- and bimetallic noble metal zirconia catalysts, *Catalysis Letters* 115 (2007) 70-78.
- VI A. Gutierrez, R. Karinen, S. Airaksinen, R. Kaila, A.O.I. Krause, Autothermal reforming of ethanol on noble metal catalysts, *International Journal of Hydrogen Energy* 36, (2011) 8967-8977.

CONTRIBUTIONS

The author's contributions to the appended papers are as follows:

- I The author planned the research, prepared the catalysts, carried out the testing and part of the characterization of catalysts, and with the co-authors interpreted the results and wrote the manuscript.

- II The author planned, carried out part of the experiments, interpreted the results and wrote the manuscript together with the main author.

- III, IV The author prepared the catalysts and carried out part of the experiments, interpreted the results and characterization results together with the main author and contributed to the writing of the manuscript.

- V The author participated in the preparation of catalysts and contributed to the interpretation of results and writing of the manuscript.

- VI The author carried out part of the experiments and was the main contributor in the interpretation of the results and writing of the manuscript.

Abbreviations and symbols

4,6-DMDBT	4,6-Dimethyldibenzothiophene
ATR	Autothermal reforming
BET	Brunauer–Emmett–Teller (calculated specific surface area from adsorption isotherm)
BTL	Biomass to liquids
C_{in}	Carbon in hydrocarbon feed
CAT	Cathechol, 1,2-dihydroxybenzene
CE	Capillary electrophoresis
CHP	Combined heat and power
CRA	Catalytic cracking
CRE	Cresol, methylphenol
CST	Crude sulfate turpentine
CTO	Crude tall oil
D	<i>n</i> -Dodecane
DCO	Decarboxylation
DDO	Deoxygenation
DMDS	Dimethyldisulfide
DME	Demethylation
DMO	Demethoxylation
DR	Dry reforming
DRIFT	Diffuse reflectance Fourier transform infrared
EDX	Energy dispersive X-ray
EU	European Union
F	Molar flow
FAME	Fatty acid methyl ester
FFA	Free fatty acid
FID	Flame ionization detector
FT	Fischer-Tropsch
FT-IR	Fourier transform infrared (spectroscopy)
GC	Gas chromatography
GHG	Green house gas
GPC	Gel permeation chromatography
GUA	Guaiacol, 2-methoxyphenol
H	<i>n</i> -Heptane
H/C	Hydrogen to carbon atomic ratio
HC	Hydrocarbons
HDO	Hydrodeoxygenation
HDS	Hydrodesulfurization
HPLC	High performance liquid chromatography
HPTT	High pressure thermal treatment
HYC	Hydrocracking
HYD	Hydrogenation
ICP-MS	Inductively coupled plasma–mass spectrometry
ICP-OES	Inductively coupled plasma–optical emission spectrometry
m	Mass
MCH	Methylcyclohexane

MCT	Mercury-cadmium-telluride
Met-CAT	Methylcatechol
MS	Mass spectrometry
MSR	Methane steam reforming
M_w	Molecular weight
n	Mol or number of atoms
NG	Natural gas
NL	Normal liters
NMR	Nuclear magnetic resonance
NTP	Normal temperature and pressure
O/C	Oxygen to carbon atomic ratio
OX	Oxidation
P	Product distribution
P	Pressure
PHE	Phenol
PO	Pyrolysis oil
POX	Partial oxidation
R	Gas constant
RA	Rosin acid
Ref/Ox	Reforming to oxidation molar ratio
SEM	Scanning electron microscopy
STR	Steam reforming
T	Toluene
T	Temperature
TCD	Thermal conductivity detector
TGA	Thermogravimetric analysis
TPO	Temperature programmed oxidation
TPR	Temperature programmed reduction
V	Volume
VTT	Technical Research Center of Finland
WGS	Water gas shift
X	Conversion
XPS	X-ray photoelectron spectroscopy
XRD	X-ray diffraction
XRF	X-ray fluorescence
Y	Yield
y	Molar fraction

1 Introduction

The energy demand is increasing in the world. In the past few years the price of crude oil has risen. This together with the need to ensure energy security, the concern about trade balance, the desire to decrease greenhouse gas (GHG) emissions, and the potential to benefit rural areas, are the main reasons why governments are showing interest in biofuels [1,2]. While several renewable alternatives are available for the production of electricity, e.g., solar energy, wind power, and hydrogen, biomass is the only renewable source that can meet the demand for carbon-based liquid fuels and chemicals [3].

Biomass is any renewable organic matter such as agricultural crops, crop residues, wood, animal waste, animal fat, municipal waste, aquatic plants, and fungal growth. These materials can be used for the production of liquid fuels and chemicals. The technology applied depends on the type and complexity of the biomass, and the end products. The liquid or gaseous fuels produced from biomass are known as biofuels and these fuels can be used in stationary (electricity and heat) and mobile applications (ships and cars) [4].

Biofuels can be classified into first- and second-generation. First generation biofuels are bioethanol produced from sugar, starch, wheat, potatoes, and maize via fermentation [5], biodiesel produced from transesterification of vegetable oils, fats and waste streams, and biomethane produced from upgrading of biogas or landfill gas. The main feedstocks used in the production of first generation biofuels are part of the food chain and therefore they are not the best alternative in a world where food availability is challenging. However, they have the main advantage that they are produced with today's available technologies [6].

Second generation biofuels are alcohols and synthetic biofuels produced from lignocellulosic biomass (short-rotation wood crops or forest residues, algae, organic waste, etc.), hydrogenated vegetable oils or used vegetable oils, and industrial residues or waste streams. It is expected that second generation biofuels will be produced effectively in large production facilities. However, as their technologies are still under development, it remains to be proved whether these fuels will have a better energy, economy, and carbon performance than first generation product pathways. [6]

First and second generation biofuels will help to increase the energy efficiency and improve the short-term energy sources in Europe [7]. However, vehicle and component manufacturers, transport providers, the energy industry, and householders are looking at alternative energy sources and fuels that are more efficient and cleaner than fossil fuels and biofuels. Hydrogen (including hydrogen produced from biomass-derived liquids) or hydrogen-rich mixtures (synthesis gas) can be used as fuel because of their clean combustion, the possibility of long-term storage of the primary fuel, and the diversity of primary fuels that can be used in their production, e.g., natural gas, biomass, and crude oil. [7,8,9] In long term, a hydrogen-based economy could therefore provide energy security. In this scenario, biomass will still be the source of carbon for chemicals. To overcome the increasing energy demand and to ensure energy security, countries are looking for alternatives based on their natural resources.

1.1 The European Union and the environment

According to the European Union (EU), 21% of all the GHG emissions that contribute to global warming are coming from transport. Furthermore, nearly all the fuel used in the transport sector comes from crude oil. Oil reserves are limited in the EU. It is thus essential to find alternatives for reducing the emissions from transport and secure energy supplies for the future, thereby reducing the dependency on oil imports. [10]

To achieve this, the EU has already taken actions. These include legislation supporting the production and use of biofuels, operating closely with the vehicle manufacturers to develop new models that are cleaner and more fuel-efficient than conventional vehicles, and improving public transport and encouraging the use of environmentally-friendly modes of transport where possible [10].

There is great potential for the production of biofuels in Europe. The EU promotes the use of sustainable biofuels, which generate clear savings in GHG emissions without negative impact on biodiversity and land use. The EU directives target a 10% share of energy from renewable fuel in transport by 2020 [11], and according to visions for 2030, the value should reach 25%. [12]

The targets set by the EU have not been reached so far. Therefore, innovative technologies are needed to produce biofuels from a wide range of biomass at low cost and in an energy-efficient way.

1.2 Energy sources in Finland

Forest covers 86% of the Finnish land area, making Finland the most extensively forested country in Europe [13]. In 2012, Finland imported 50% of the total primary energy – oil, coal, and natural gas [14]. In the same year, 25% of the energy consumption was from renewable energy sources, i.e. the third highest value in Europe [11,15]. As shown in Figure 1, significant local energy sources are wood, peat, hydropower, and wind energy. Wood is the most utilized energy source and as the Finnish forest is growing by about 105 million cubic meters each year [16], it is expected that forest resources will also be used to a larger extent in the future as a source of carbon for liquid fuels and chemicals.

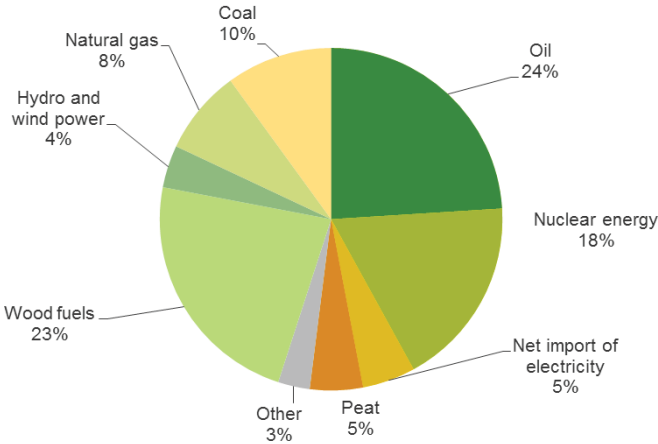


Figure 1. Energy sources in Finland in 2012. Total energy consumption in 2012 1.36 PJ (petajoule) or 380 TW (terawatt hours). [15]

1.3 Wood as raw material for fuels

Wood is the fibrous structural tissue found in stems and roots of trees and other woody plants. It has been utilized as fuel and construction material for nearly all of human history [17]. Our planet has about one trillion tons of wood. The growth rate is 10 billion tons per year. As it is abundant, carbon-neutral, and does not compete with the food chain, wood has been of interest as a source of renewable energy. [16,18]

The composition of wood varies depending on the tree species. The main components of wood are cellulose (39-45 wt-%), hemicelluloses (19-33 wt-%), lignin (22-31 wt-%), and extractives (2-4 wt-%). [19]

Wood has different industrial applications, e.g., fibers are used in the production of pulp, paper, and composites, logs for sawn goods and plywood, bark and branches can be used in the production of energy and second-generation diesel via biomass to liquid (BTL). Lignin is used as energy source but new applications are also being developed, e.g., in the production of fuels and chemicals.

2 Conversion of wood to fuels

Different technologies are available for the conversion of wood to liquid and gaseous fuels. Main technologies involving wood as feedstock are presented in Table 1. These technologies include fermentation of sugars from wood to ethanol, and thermal technologies such as gasification and pyrolysis. The high organic content of waste or side streams from Kraft pulping can be utilized, for example, crude tall oil (CTO) and crude sulfate turpentine (CST) can be used for the production of fuels.

Table 1. Process for the conversion of wood to liquid, gas, and solid fuels. [20,21,22]

Process	T (°C)	Atmosphere	Products	Mean overall yield (product/ton biomass, %)
Fermentation	30-35	Air	Ethanol	20 – 25
Combustion	> 900	O ₂ (air)	CO ₂ + H ₂ O + N ₂ + ashes to be treated	~ 65
Pyrolysis (slow pyrolysis)	< 700	Inert gas, low pressure	Char + tar + gas, which proportions are related to the pyrolysis parameters	~ 45
Gasification	>800	Air or H ₂ O vapor	Gas (H ₂ , CO, CO ₂ , CH ₄ , N ₂) + ashes to be treated	50 – 60
Fast pyrolysis	<550	Inert gas, low pressure	High viscosity liquid (phenols)	~75
Direct liquefaction	300 – 350 slurry in water	CO high pressure	High viscosity liquid (phenols) non-soluble in water	~80

2.1 Fermentation process

Although the fermentation of sugars from crops such as corn or wheat to ethanol is well known, the drawback of these processes is that the raw materials compete with the food chain, as discussed in the introduction [5]. Lignocellulosic biomass such as hard- and softwood residues can be used as sugar sources for ethanol production [23]. However, the process to release the sugars from lignocellulosic biomass is more complicated than that utilized for starchy biomass. The process also generates by-products that inhibit the fermentation. For this reason, the production of cellulosic ethanol is complicated and expensive. [24]

In general, the average fermentable sugars from wood constitute approximately 50 wt-% of the original dried wood [20] as cellulose and solid lignin can be converted to sugars by either acid or enzymatic hydrolysis [25]. The production of ethanol from wood starts with the pretreatment of the wood. The pretreatment is performed to decrease the crystallinity of cellulose, increase the surface area of the wood, remove hemicellulose, and break the lignin [25]. The pretreatment can be physical, chemical, and thermal or a combination of the three. This step is followed by the hydrolysis of the material to a variety of sugars that are suitable for ethanol production. Although a large variety of sugars are present after the hydrolysis, only some can be fermented by the standard yeast that is used in the ethanol industry [23].

According to the EU standard EN 228, ethanol can be used as a 5% blend in gasoline. No engine modifications are required for this blend. However, if the engine is modified, for example, blends containing up to 85% of ethanol (E85) can be used. [5]

Ethanol can also be utilized as a source of hydrogen. When ethanol is reformed in the presence of a suitable catalyst and appropriate operation conditions, synthesis gas (mixture of hydrogen and carbon monoxide) or hydrogen-rich gas is obtained that can be fed to fuel cells for electricity production. [26]

2.2 Thermal processes

The thermal technologies (combustion, gasification, and pyrolysis) listed in Table 1 yield gases, char, ashes, and liquids as products. However, none of the technologies presented yields a product that is similar to conventional transport fuels, whereby further treatment is needed.

The products from combustion are carbon dioxide and steam. In the case of biomass combustion the resulting carbon dioxide was previously captured by plants, and the overall process is therefore carbon-neutral. Biomass can be combusted to produce electricity and CHP (combined heat and power) via a steam turbine in dedicated plants. Modern CHP plants working at a maximum of 540 °C can yield an electrical efficiency of 33% to 34% (low heating value), even up to 40%, if operated in electricity-only mode. [27]

In the case of gasification, biomass is converted mainly to carbon monoxide, hydrogen and light hydrocarbons (HC). When this technology is combined with the Fischer-Tropsch (FT) synthesis and treatment of the FT product, HC in the range of gasoline and diesel are obtained. The overall yield from wood (1 ton) to FT diesel (~210 liters), is approximately 20% and the energy efficiency for tree-to-barrel is about 44% [22]

The energy consumption for pyrolysis is expected to be lower than for gasification as the breakdown of chemical structures in pyrolysis is not as extensive as in gasification. Depending on the residence time of the feed in the pyrolyser, pyrolysis processes can be divided into slow and fast. Slow pyrolysis (5-30 minutes at 600 °C) yields charcoal as the main product, while fast pyrolysis (0.5-5 seconds at 400-550 °C) yields mainly a liquid product. Thermal breakdown of structures present in wood into smaller chemical substances occurs at the temperatures used in fast pyrolysis. The pyrolysis process produces typically 70-75 wt-% liquid (pyrolysis oil, PO), 15 wt-% combustible gas, and 15 wt-% char [28]. PO is a complex mixture of oxygen-containing compounds. The main advantage of fast pyrolysis is that the pyrolysis oil has a higher energy density than the starting wood making the oil more suitable for industrial applications. [29,30,31]

2.3 Wood-based pyrolysis oils

The products of the pyrolysis of wood or forest residues, the so-called wood-based POs, contain large quantities of oxygen-containing compounds (carboxylic acids, aldehydes, ketones, carbohydrates, and thermally degraded lignin), water, and alkali metals. The oxygen-containing compounds (40-50 wt-%) and the large water content (15-30 wt-%) make wood-based POs chemically and physically unstable. Although wood-based POs have a higher energy density than wood, they are acidic (pH~2) and incompatible with conventional fuels. Furthermore, wood-based POs have a high viscosity and a high solid content. [30]

The properties mentioned above make the engine application of wood-based POs challenging. In the 90s Wärtsilä performed engine tests in the 4R32 engine with wood-based PO [32]. However, the conclusion was that wood-based PO operation requires further research and development which was not justified with regard to the market outlook at that time.

Further processing is required to improve chemical and physical properties of wood-based POs. The composition of POs depends on the biomass used but they have the main advantage of being sulfur-free or having low sulfur content (< 40 ppm). [12,33,34,35]

2.3.1 Upgrading

Upgrading of wood-based POs (empirical formula $C_6H_8O_4$ based on the elemental analysis of wood-based POs) is performed to remove or convert at least part of the oxygen-containing compounds into less reactive functionalities in order to improve the physical and chemical properties [33,34,35,36]. The upgrading can be performed thermally or catalytically. Thermal upgrading refers to the treatment of the oil at high temperatures in different gas atmospheres. Miguel de Mercader et al. [37] have carried out extensive research on the thermal upgrading of PO in nitrogen and hydrogen atmospheres obtaining oils that were suitable for further treatment in a conventional refinery. Catalytic upgrading

includes decarboxylation (DCO, Eq. 1), catalytic cracking (CRA, Eq. 2), hydrodeoxygenation (HDO, Eq. 3) or a combination of these [33].



DCO (Eq.1) is performed on zeolites [3,33]. In DCO, oxygen is removed in the form of carbon dioxide, thus there is loss of valuable carbon into the gas phase. The overall theoretical carbon yield calculated on the basis of dried wood and Eq. 1 is approximately 23 wt-% (carbon in hydrocarbon product/carbon in wood). CRA (Eq. 2) is also performed over zeolite [33]. In this reaction, the oxygen present in the wood-based PO is removed as water and carbon dioxide. However, the carbon loss is less than in DCO, as the overall theoretical carbon yield is approximately 27 wt-%. The product is expected to be aromatic and there is the risk of extensive cracking of long chain HC and thus increasing the amount of light HC in the gas phase [33]. In HDO (Eq. 3), oxygen is removed as water so, carbon loss will in principle not occur [33]. The overall carbon yield for HDO is 35 wt-%. HDO is similar to well-known desulfurization processes at the oil refinery which utilize sulfided, Al₂O₃-supported CoMo and NiMo catalysts. The main disadvantage of HDO is the large amount of hydrogen needed to achieve complete oxygen removal. In a real process where hydrogen is present, the reactions take place in combination so that, even though one might predominate, the others are also present. Thus, a difference is expected between the theoretical and the real carbon yields.

The low carbon loss into the gas phase and therefore, the large amount of liquid product together with the available knowledge on how to operate the HDO process, make HDO promising for the upgrading of wood-based PO.

As seen for DCO (Eq. 1), CRA (Eq. 2), and HDO (Eq. 3), catalytic processes are an alternative for the upgrading of wood-based POs. However, the highly reactive oxygenates and the presence of water bring about challenges for the catalysts that have been developed for the petroleum industry, where the feedstocks have only low concentrations of oxygen-containing compounds and water. [38,42]

2.3.2 Hydrotreatment

In this thesis hydrotreatment refers to the catalytic processes used for the partial or complete removal of oxygen-, nitrogen-, and sulfur-containing compounds, and hydrogenation (saturation of double bonds and aromatics) from, e.g., wood-based POs, in the presence of hydrogen at high temperatures (up to 450 °C). The reduction of oxygen-containing compounds or the change in the oxygen containing functionalities yields a product that has better fuel properties, e.g., chemical and physical stability and energy value than the starting wood-based PO [36,39,40,41]. The removal of oxygen occurs in the form of water, but carbon dioxide, carbon monoxide, and methane are also formed. This indicates that at real process conditions several reactions take place simultaneously or in parallel, e.g., hydrogenation (HYD, saturation of double bonds), DCO (Eq. 1), and CRA (Eq. 2). The large amounts of water formed cause the separation of the product into an organic and a water phase [12,42].

Possibilities for the conversion of biomass to fuel components including hydrotreatment are presented in Figure 2. Hydrotreatment can be used to improve the quality of vegetable oils, carbohydrates, products from cellulose, and hemicellulose so that they can be used as components for gasoline and diesel [43,44,45]. Hydrotreatment is already available commercially. Neste Oil has developed and commercialized the process known as NExBTL in which various feedstocks such as vegetable oils are converted to a high quality diesel component [46]. UOP developed and commercialized the hydrotreatment processes UOP/Eni Ecofining™ and the Honeywell Green Jet Fuel technology [47,48].

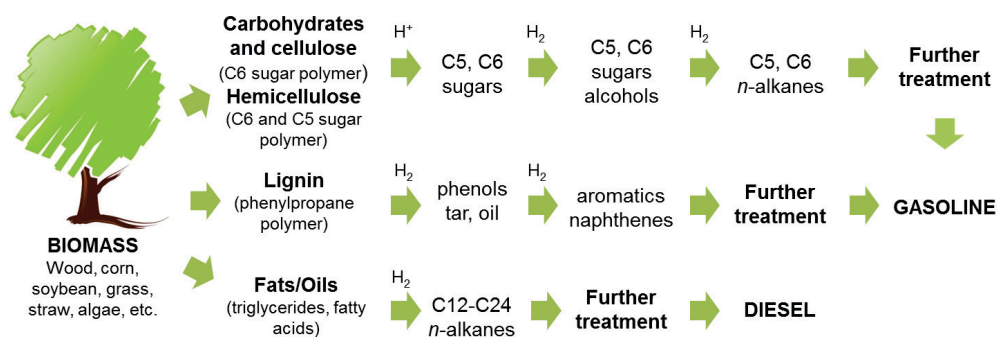


Figure 2. Hydrotreatment of biomass building blocks to hydrocarbon. Adapted from [49].

Under the conditions of hydrotreatment of wood-based POs, lignin and compounds produced in the thermal degradation of lignin, such as guaiacol (GUA, 2-methoxyphenol),

substituted guaiacols and carbohydrates, tend to form heavy HC and carbonaceous deposits reducing the activity of the catalyst [50,51].

Large amounts of hydrogen are needed to completely remove oxygen (oxygen-free product); this high hydrogen consumption is a disadvantage in the hydrotreatment of PO [33]. A reaction scheme proposed based on experiments performed with wood-based PO is presented in Figure 3 where the main reactions are re-polymerisation, HYD, HDO, and HYC (hydrocracking) (Eq. 3). The operation conditions and the presence of a catalyst play an important role in the upgrading, as different temperatures favor different reactions. At temperatures higher than 80 °C in the presence of hydrogen and a catalyst the formation of saturated oxygen-containing compounds is favored. At temperatures higher than 175 °C, however, the catalytic reaction competes with re-polymerization which is a non-catalytic reaction. The high-molecular-weight product formed in re-polymerization can be hydrogenated in the presence of a catalyst and at the suitable temperature and hydrogen pressure, yielding non-polar fragments and an aqueous phase. [52]

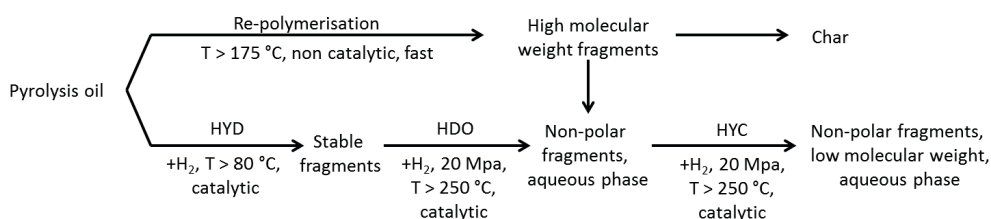


Figure 3. Reaction path for pyrolysis oil upgrading. [52]

2.3.3 Hydrotreatment catalysts

Sulfided Al_2O_3 -supported CoMo and NiMo catalysts are used in oil refineries in hydrotreating processes, where removal of S, N, O, and metals from oil streams and saturation of HC take place. These conventional catalysts are easily available at a reasonable cost. [53,54]

Sulfur releases from the surface of the sulfided catalyst can take place in hydrotreatment and cause the deactivation of the catalyst and contamination of the product [42,55,56]. As wood-based PO has a low sulfur content, a sulfiding agent is needed to keep the sulfided

catalysts in the active form and extensive sulfur stripping is required to obtain a sulfur-free product [43,57,58,59,60].

Other deactivation mechanisms of sulfided Al_2O_3 -supported CoMo and NiMo catalysts are [54]: sintering of the active site, covering of the active phase by reactants or products, and deposition of carbonaceous materials. The formation of carbonaceous deposits that deactivate the catalysts is favored by the Al_2O_3 support which is known to coke due to its acidic nature [36,51,61].

Large amounts of water are present in the bio-derived liquids, and water is also produced during hydrotreatment [62,63]. Water vapor has been reported to cause recrystallization of the $\gamma\text{-Al}_2\text{O}_3$ support into hydrated boehmite and to partially oxidize the nickel sulfide phase, resulting in decreased activity [64]. Consequently, the large scale application of these Al_2O_3 -supported catalysts in hydrotreatment of PO is challenging. The performance of the sulfided Al_2O_3 -supported CoMo and NiMo catalysts can be improved for example by changing the support to a less acidic one, e.g., active carbon, silica (SiO_2), titania (TiO_2) or zirconia (ZrO_2) [36,65]. Another alternative is to replace the conventional sulfided catalysts with more suitable ones that tolerate water and exhibit limited activity in coke formation reactions.

Metals such as Ni, Pd, Pt, and Cu on a support are known to be good hydrogenation catalysts. Reduced transition and noble metal catalysts are active in the hydrotreatment at lower temperatures than those required by conventional sulfided catalysts, lowering the extent of thermal cracking and minimizing the formation of carbonaceous deposits. Furthermore, transition and noble metal catalysts can also be produced on supports that exhibit a higher water tolerance than Al_2O_3 , such as TiO_2 , ZrO_2 or activated carbon. [42,33, 62,66]

2.3.4 Guaiacol as model compound

The large amounts of chemical compounds present in wood-based POs make necessary the use of model compounds for proper understanding of the system. The knowledge gathered with model compounds cannot, however, always be transferred easily to real feedstocks. Working with model compounds makes the analysis and quantification of

feeds and products easier. Furthermore, it allows the identification of reactions possibly taking place under the conditions used with the real feed, identification of reaction intermediates, and the reaction scheme for some compounds present in the real feed.

Lignin is a polyaromatic compound consisting of polymers of coniferyl alcohol, sinapyl alcohol, and coumaryl alcohol [67]. During the pyrolysis of wood, lignin decomposes thermally into smaller-molecular-weight fractions. These lignin fractions are likely to coke under the conditions used for PO upgrading [36,40,50,]. Among the most studied compounds for the lignin fraction of wood-based pyrolysis oils are GUA or substituted GUAs at different temperatures and pressures on sulfided NiMo and CoMo catalysts [36,40,65]. The aim in these previous works has been to predict the behavior of the lignin fraction at the conditions used for the hydrogenation of wood-based POs. However, non-sulfided catalysts are desired for this application since wood-based POs are almost sulfur-free, and sulfur leaching from the sulfided catalyst may contaminate the product with sulfur [3,63], as will be discussed in more detail in Chapter 2.3.4.

Several authors have reported reaction schemes of GUA with different degree of complexity under hydrotreatment conditions. One of the most recently published reaction schemes for the reactions of GUA at 300 °C and 9 MPa on a sulfide catalyst is presented in Figure 4. The reactions of GUA under these conditions include demethylation (DME) of GUA to catechol (CAT, 1,2-dihydroxybenzene), demethoxylation (DMO) of GUA to phenol (PHE), deoxygenation (DDO or HDO) of PHE to benzene and HYD of PHE to cyclohexanone. Condensation reactions in the reactions of GUA lead to heavy products which could deposit on the catalysts and have a negative effect on the activity [65].

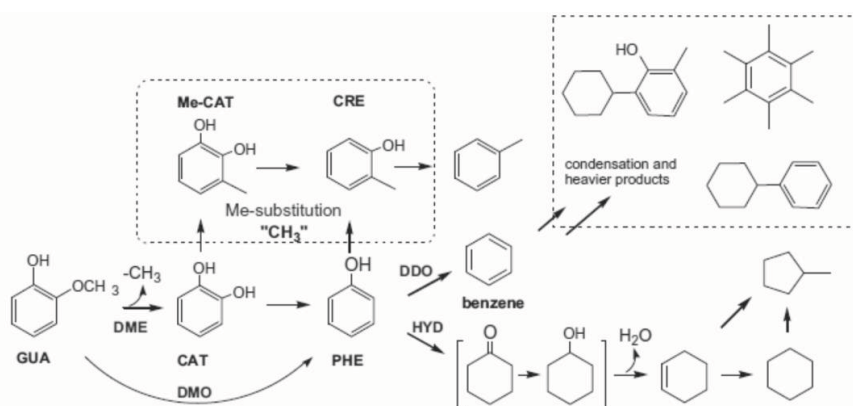


Figure 4. General reaction scheme for guaiacol on sulfided CoMo/Al₂O₃ at 300 °C and 9 MPa. DME: demethylation, DMO: demethoxylation, DDO: deoxygenation, HYD: hydrogenation, GUA: guaiacol, CAT: catechol, Me-CAT: methylcatechol, CRE: cresol, PHE: phenol. [65]

2.4 Side streams from pulping process to fuels

The most important by-products of the kraft pulp industry are CTO and CST. These by-products are used after refining in the paint industry and also for other purposes [68]. Figure 5 gives a schematic representation of a pulping process [69]. The amounts of CTO and CST produced during the kraft pulping process depend on the wood material and the storage of the wood. The yield of CTO in the pulping process is in the range of 20-50 kg/ton pulp and the yield of CST is 10 kg/ton of pulp [70].

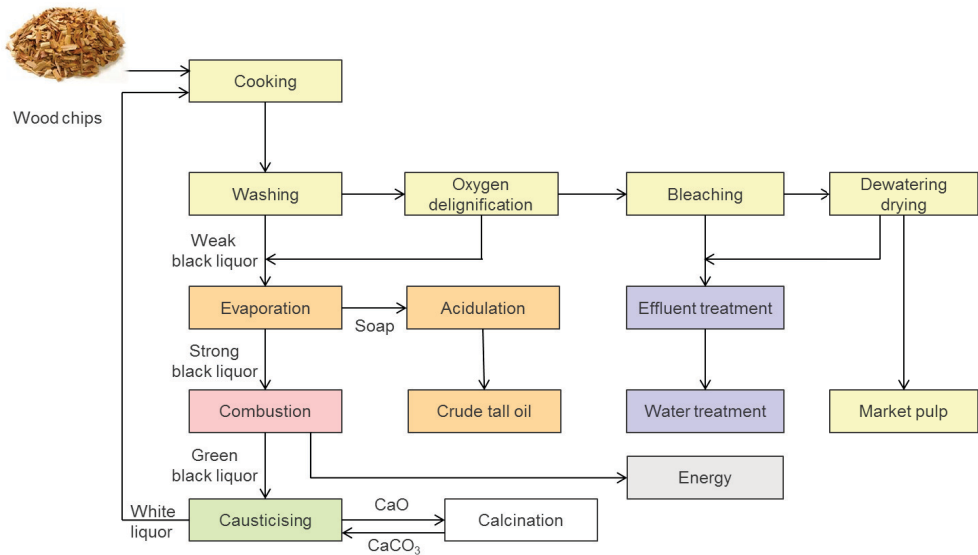


Figure 5. Schematic presentation of a pulping process. [69]

2.4.1 Crude tall oil

CTO is a mixture containing 36-58% of free fatty acids (FFAs) with a hydrocarbon chain of 16 to 20 carbons with C₁₈ dominating, 10-42% of rosin acids (RAs), abietic acid being the dominant one in this group, and 10-38% of sterols and neutral substances, β -sitosterol being predominant. [70,71] FFAs and RAs can be separated by vacuum distillation. The

residue, tall oil pitch, can be used as a source of phytosterols or simply utilized for energy production [70].

There are different ways of processing CTO to HC; these include esterification, hydrotreatment, and deoxygenation [70]. Esterification of FFAs with methanol yields FAMEs (fatty acids methyl esters). Mikulec et al. [70] demonstrated that CTO is amenable to esterification without any pretreatment. After a 4 to 5-hour reaction, vacuum separation of the unreacted methanol and the formed water resulted in a 48-52 % yield (tall oil fatty acid methyl esters relative to CTO feed).

Hydrotreatment of FFAs and RAs from CTO on commercial CoMo, NiMo, and NiW catalysts has been studied [70]. The applied hydrogen pressure is around 5-10 MPa, the temperature from 250 to 400 °C. After the hydrotreatment, the product was fractionated into gasoline and diesel fractions. The CTO diesel is a high-quality fuel that can be used as a blend with regular diesel fuel oil.

Catalytic deoxygenation of CTO on supported noble metal catalysts has also been studied. Metal-catalyzed deoxygenation in a hydrogen-free atmosphere is an effective way of producing liquid fuels. [70,72,73,74]

2.4.2 Crude sulfate turpentine

CST is a by-product of the kraft pulping process and is extracted mainly in the same step as CTO. CST is a mixture of volatile unsaturated C₁₀H₁₆ terpene isomers derived from pitch. The average composition of CST is 50-60% of α -pinene, 20-30% of Δ^3 -carene, the rest being other terpenes. The large concentration of volatile sulfur containing compounds (1-3% as S) and the high chemical reactivity of the α -pinenes make unprocessed CST unsuitable as fuel or biocomponent. [75]

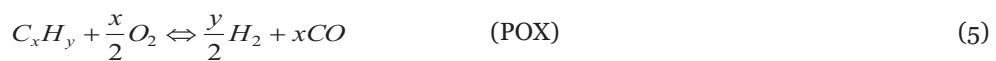
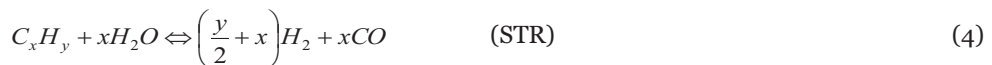
Turpentine can be hydrogenated on catalysts similar to CTO (Al₂O₃-supported CoMo and NiMo) at pressures between 1 MPa and 5 MPa and temperatures between 200 °C and 400 °C. The process yields a sulfur-free light hydrocarbon fraction that can be mixed with gasoline. [75]

3 Production of bio-based synthesis gas

The conversion of HC to hydrogen or syngas (synthesis gas, mixture of hydrogen and carbon monoxide) has gained importance. These are used in large-scale production plants utilizing gas-to-liquids processes (FT synthesis) and also in refineries where large amounts hydrogen are needed, as well as in small units such as fuel cells for automobile applications. Because of their clean combustion, the possibility of long-term storage of the primary fuel and the diversity of primary feedstocks (natural gas, biomass, ethanol, crude oil, etc.) that can be used in their production, hydrogen or hydrogen-rich mixtures, e.g., syngas, can be used as fuel. [7,76,77,78]

3.1 Main reactions of hydrocarbons

Owing to its high electrochemical reactivity, hydrogen is the preferred feedstock for fuel cells compared with HC or alcohols [79]. Hydrogen can be produced by different methods [80]: catalytic, including steam reforming (STR) of HC, electrochemical, photochemical, and biological. An interesting approach is autothermal reforming (ATR), a combination of STR and oxidation (OX) reactions [8,9]. Here, the energy required by the endothermic STR reaction is provided by the exothermic OX reaction. The main reactions taking place in ATR are presented below; STR (Eq. 4), POX (partial oxidation, Eq. 5), DR (dry reforming, Eq. 6), and OX (complete oxidation, Eq. 7).





Using ethanol for the production of syngas, gives rise to many reactions. The main reactions are given below, Eq. 8 – 24. [81]

STR



DR



OX



POX



Dehydrogenation



Dehydration



Decomposition



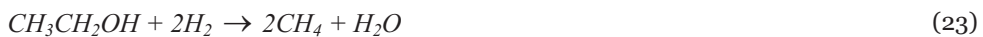
Acetaldehyde steam reforming



Acetaldehyde decomposition

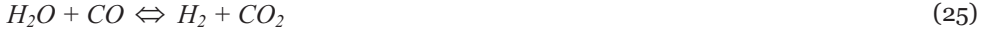


Other reactions



Some reactions, such as WGS (water gas shift, Eq. 25), MSR (methane steam reforming, Eq. 26), decomposition reaction of products (Eqs. 27 and 28), and coke formation and gasification (Eq. 29- Eq. 33) are shared by the ATR of HC and ATR of ethanol.

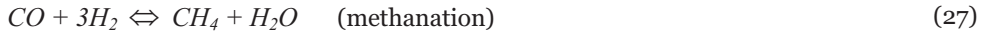
WGS



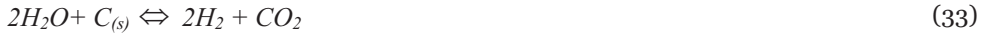
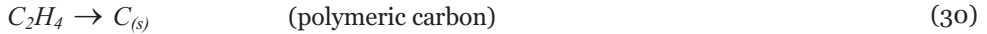
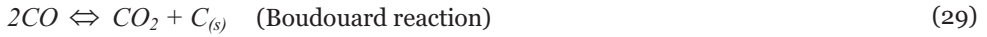
MSR



Reaction of decomposition products



Coke formation and gasification



Unfortunately, there is a lack of infrastructure for hydrogen production and especially for hydrogen distribution for automobile applications (fuel cells). Therefore, the use of on-board fuel processing technology for reforming of gasoline, diesel, methanol, and ethanol to generate hydrogen is very promising. In the case of on-board reforming of conventional fuels the infrastructure for the production and distribution of gasoline and diesel could be applicable [82]. Fossil diesel and also biofuels, e.g., second generation diesel fuels have the advantage of high hydrogen density as they are mixtures of saturated HC. Accordingly, model compounds or mixtures of model compounds are used to simulate the reforming of real fuels. Working with model compounds helps, among other things, to identify reactions taking place and the catalyst performance. Ethanol could also be used as hydrogen source for mobile fuel cell applications because it has a high hydrogen density and can be produced in the fermentation of biomass.

3.2 Commercial catalysts

Hydrogen is commercially produced by STR of natural gas (NG) using supported Ni catalysts. Large amounts of carbonaceous deposits are formed during the operation, resulting in a rapid deactivation of the catalyst and an increase in the reactor pressure. For this reason, the process must be stopped and the catalyst regenerated. [83,84]

Commercial Ni catalysts are usually supported on modified alumina, which is an acidic substance. The support of the reforming catalyst plays an important role, because acidic materials are believed to promote the dissociation of the hydrocarbon on the sites at the periphery of the metal crystallites (metal-support interface). [85]

In the STR of conventional “sulfur-free” fuels, the catalysts must be tolerant to the low amount of sulfur (< 5-10 ppm) that remains after the hydrodesulfurization (HDS) process. Dialkylbenzothiophenes are highly resistant to HDS due to the steric hindrance of the alkyl group that prevents the contact between the thiophenic sulfur atom and the active site of the HDS catalyst. Low levels of sulfur are known to poison Ni catalysts [82,86]. Adding noble metals to Ni or using other metals proved to overcome this problem. NiSr/ZrO₂, NiRe/Al₂O₃, NiPt/Al₂O₃, Ru/Al₂O₃, Ni/CeZSM-5 have been shown to be active in the STR of liquid HC for long periods of time [87].

Noble metal catalysts, in particular Rh, are active in the reforming of HC [82]. The advantage of Rh is that it is more active towards STR than OX reactions [88,89]. The high reforming activity of Rh is followed by Pt and Pd. This high activity allows using a low metal loading, which is very important considering the high price of these metals. [90]

4 Noble metal catalysts

The combination of Rh, Pt, and Pd is used in cars as exhaust gas cleaning catalysts (three-way catalyst). Attempts have been made to replace them by cheaper metals, e.g., Cu, Cr, Fe, Co, and Ni oxides, but automotive exhaust treatments still continue to rely upon them. In three-way catalysts Rh, Pd, and Pt are used to promote the oxidation of carbon monoxide to carbon dioxide and the complete oxidation of HC to carbon monoxide and water, and the high conversion of nitrogen oxides (NO_x) to nitrogen over a wide range of conditions. [91]

Rh catalysts are used in hydrogenation, selective hydrogenation, carbonylation, reductive amination, and oxidation reactions. Pd is used in hydrogenation, selective hydrogenation, oxidation, dehydrogenation, hydrogenolysis, dehalogenation, carbonylation, and disproportionation/migration of olefins. Pt is used in hydrogenation, oxidation, dehydrogenation, isomerization, hydrogenolysis, and reductive alkylation. [92,93]

Pt has the advantage of being resistant to aging at high temperatures under oxygen-rich conditions, making it suitable for ATR where high temperatures and an oxygen atmosphere are used. [91]

Similarly to the other noble metals, Pd has the advantage that its activity can be improved by changing the support and by alloying it with other metals [94]. For instance, the addition of Cu to Pd increases the hydrogenation activity of Pd. [95]

The support material of the catalyst is important as this material substantially modifies the chemical behavior of the dispersed metal [96,97,98]. The support materials must be thermally stable at the high temperatures used, be resistant to thermal shock, and inclusion of metal particles should not be possible [89,99]. Al_2O_3 is a commonly used catalyst support. Al_2O_3 is known to enhance cracking reactions and catalyst deactivation through carbon deposition. This cracking and deactivation is attributed to the acidity of Al_2O_3 [99]. Thus, neutralizing the acidity of the support by using a less acidic material such as ZrO_2 or oxide-stabilized ZrO_2 provides options to reduce the carbon deposition [100]. The lower acidity of ZrO_2 makes it less active in carbon deposition reactions than

Al_2O_3 [101]. Furthermore, ZrO_2 -containing materials also possess high thermal stability [102,103,104]. One of the disadvantages of ZrO_2 is, however, its low surface area obtained after calcination at elevated temperatures [102,104].

Al_2O_3 has been reported to interact detrimentally with Rh causing a decrease in the amount of surface Rh after a treatment at high temperatures in an oxidizing atmosphere [104]. This interaction between Rh_2O_3 and the Al_2O_3 support can cause deactivation of the catalysts. Fortunately, this interaction is not detected with ZrO_2 , making ZrO_2 an interesting option for Rh support. Magnesium oxide (MgO) or other oxides serve as alternatives for the Al_2O_3 support as these materials provide both stability and suitable surface area for ATR reactions. [99,104,105]

Noble metal catalysts exhibit a better tolerance to sulfur than conventional reforming Ni catalysts [106]. The support is also known to play an important role as certain materials, e.g., CeO_2 could adsorb sulfur and in most cases this reaction is more favorable than the interaction between sulfur and the active metal. The acidity of the support also plays an important role in the sulfur tolerance of the catalyst. Therefore, the bifunctionality of ZrO_2 makes it promising for the treatment of sulfur-containing feedstocks [107,108].

The price of noble metal catalysts is a serious drawback that could limit their application. Therefore low metal concentrations (< 1 atomic-%) are typically utilized on an industrial scale [109,110].

5 Scope of the research

Pyrolysis oils are complex mixtures of oxygen-containing compounds. These compounds bring about limitations to their storage and use as fuels. Their properties can, however, be improved in the presence of a catalyst at high hydrogen pressures and high temperatures (discussed in Chapter 2.3.1). The use of commercial sulfided catalysts is challenging, as large amounts of carbon deposits are formed on the catalyst. In addition, sulfur leaching from the catalysts causes severe decrease in the activity and stability of the sulfided Al_2O_3 -supported CoMo and NiMo catalysts and contaminates the product that would otherwise be sulfur-free (discussed in Chapter 2.3.4). Hydrogen-rich gas mixtures can be produced in the autothermal reforming of liquid hydrocarbons. The use of commercial Ni/ Al_2O_3 in these reactions is limited because the carbon deposition causes plunging of the reactor and increases the pressure drop over the reactor (discussed in Chapter 3.2).

The purpose of this thesis was to develop and test new catalysts to overcome the limitations of conventional hydrotreatment and autothermal reforming catalysts. Noble metal catalyst could tolerate the harsh conditions present at the hydrotreatment of biomass-derived liquids and minimized the carbon deposition in autothermal reforming of liquid hydrocarbons. A model compounds for pyrolysis oil was used in the evaluation of the performance of the noble metal catalysts (Rh, Pd, and Pt) because of the complexity of wood-based pyrolysis oils (I). These catalysts were also tested in the ATR of model compound for gasoline, diesel and ethanol (II-VI). The performance of the developed catalysts was compared to that of commercial catalysts. The catalysts were also tested with real feedstocks (hydrotreatment tests: wood-based PO (II) and autothermal reforming tests: NExBTL renewable diesel (IV)). Attention was also paid to the formation of carbonaceous deposits and to the regeneration of the noble metal catalysts.

Because of the high price of noble metal catalysts, their application in commercial processes might be challenging. The concentration of noble metal in the catalysts was therefore kept as low as possible and the bimetallic catalysts were tested with the aim of stabilizing the catalysts and reducing the price of the catalysts significantly.

6 Materials and methods

The noble metal catalysts were prepared and their performance was tested in the following reactions: hydrotreatment of a model compound for the lignin fraction of wood-based PO (I) and wood-based PO (II) and in ATR of simulated gasoline (III), diesel (IV), commercial diesel (IV), and ethanol (VI). The performance of the catalysts was compared with the performance of commercial catalysts sulfided CoMo/Al₂O₃ for hydrotreatment and NiO/Al₂O₃ for ATR. The chemicals used in the experiments reported in this thesis are presented in Table 2.

Table 2. Gases and chemicals used in the preparation, characterization, and testing of catalysts.

Gases and chemicals	Use	Supplier	Purity	Paper
ZrO ₂	Support	MEL Chemicals		I-VI
Pt(NH ₃) ₂ (NO ₂) ₂	Precursor	Aldrich	3.4 wt-% in dilute ammonium hydroxide	I-VI
Rh(NO ₃) ₃	Precursor	Aldrich	10 wt-% Rh in > 5 wt-% nitric acid	I-VI
Pd(NO ₃) ₂	Precursor	Aldrich	12-16 wt-% Pd	I-V
CoMo/Al ₂ O ₃	Catalyst	Albemarle		I-II
15% NiO/Al ₂ O ₃	Catalyst	BASF		VI
Synthetic air	Calcination of catalyst, reactant	AGA	99.999%	I-VI
H ₂	Catalyst pretreatment, characterization, reactant	AGA	99.999%	I-VI
H ₂ S in H ₂	Catalyst pretreatment, reactant	AGA	5 vol-%	I, II, IV
N ₂	Inert, chemisorption, DRIFTS	AGA	99.999%	I-VI
Ar	Inert, TPR	AGA	99.999%	I, III-VI
O ₂	Catalyst characterization	AGA	99.999%	I, III-VI
7.4% H ₂ /N ₂	Pretreatment, DRIFTS	AGA	H ₂ 99.999%	I, IV-VI
5% CO/N ₂	Pretreatment, DRIFTS	Messer Griesheim	CO 99.999%	I, IV-VI
2-Methoxyphenol (guaiacol)	Reactant	Sigma-Aldrich	> 99%	I
DMDS	Sulfiding agent	Sigma-Aldrich	>99%	II
<i>n</i> -Hexadecane	Reactant, solvent	Sigma-Aldrich	>99%	I, III-V
Dimethylbenzene (xylene)	Solvent	Sigma-Aldrich	>99%	I
Toluene	Reactant	Riedel-de-Haën	≥99.7%	III-IV
Methylcyclohexane	Reactant	Merck	≥ 99%	III-IV
4,6-DMDBT	Additive	Aldrich	97%	IV
<i>n</i> -Dodecane	Reactant	Sigma-Aldrich	99%	III-IV
<i>n</i> -Heptane	Reactant	Fluka	≥ 99.5%	III-IV
<i>n</i> -Hexane	Solvent	Sigma-Aldrich	95%	II
CDCl ₃	NMR solvent	Sigma-Aldrich	-	II
Wood-based pyrolysis oil	Reactant	VTT	-	II
Low sulfur diesel	Reactant	Neste Oil Corp.	-	IV

6.1 Catalyst preparation, pretreatment, and characterization

Monometallic Rh, Pd, and Pt catalysts and bimetallic RhPd, RhPt, and PdPt catalysts were prepared by dry impregnation [111] or dry co-impregnation on ZrO₂ support (MEL Chemicals ECo100). The ZrO₂ was ground to 0.25–0.42 mm and calcined at 900 °C for 16 h before use. After impregnation the catalysts were dried at room temperature for 4 h and then at 100 °C overnight. Subsequently, the catalysts were calcined at 700 °C for 1 h. The total metal loading was 0.5 wt-% at the maximum. The preparation procedure is described

in detail in III, IV, and V. The commercial CoMo/Al₂O₃ and NiO/Al₂O₃ were ground and sieved to a particle size of 0.25–0.42 mm (I,II,VI). The former was used in the sulfided form (I,II).

All fresh and used catalysts were characterized by various methods: X-ray fluorescence spectrometry (XRF) was used to determine the metal loading (I-III). Chemical and physical properties were measured by chemisorption (hydrogen and carbon monoxide uptake) and physisorption (Brunauer-Emmett-Teller (BET) surface area, total pore volume) (I-III,V) and in situ diffuse reflectance Fourier transform spectroscopy (DRIFTS) (V,VI).

X-ray diffraction (XRD, III), X-ray photoelectron spectroscopy (XPS) (IV), hydrogen-temperature programmed reduction (H₂-TPR) (I,III), scanning electron microscopy (SEM) (I,III), and energy dispersive X-ray (EDX) (III) were used to assess the composition and morphology of the catalyst surface. The properties of the fresh catalysts used are summarized in Table 3.

Table 3. Properties of fresh ZrO₂-supported noble metal catalysts. (I-VI)

Catalyst	T _{cal} (°C)	Target metal loading (wt-%)	Metal loading (wt-%, XRF)	BET (m ² /g _{cat})	Total pore volume above 100 nm (m ² /g _{cat})	Irreversible chemisorption of H ₂ (μmol/g _{cat})
ZrO ₂	900	-	-	20	0.19	1.5
Rh	700	0.50	0.49	20	0.096	3.1
Rh	900	0.50	n.a	19	0.093	1.3
Pt	700	0.5	0.45	17	0.15	0.01
Pt	900	0.50	n.a	18	0.04	0.13
Pd	700	0.5	n.a	17	0.08	1.2
RhPt	700	Rh: 0.25, Pt: 0.25	Rh: 0.24, Pt: 0.22	23	0.092	4.3
RhPt	900	Rh: 0.25, Pt: 0.25	Rh: 0.25, Pt: 0.22	23	0.092	1.4
PdPt	700	-	Pd:0.14, Pt: 0.32	16	0.085	0.96
RhPd	700	-	Rh:0.25, Pd: 0.12	21	0.091	1.2

The catalyst for hydrotreatment tests were pretreated in situ at 400 °C. The noble metal catalysts were first dried in air at 1 MPa for 1 h and then reduced in hydrogen for 1 h (I,II). The sulfided catalysts were dried in air at 1 MPa for 1 h and then sulfided with 5 vol% hydrogen sulfide in hydrogen for 1 h at 1 MPa (I) and with 0.1 g DMDS in 15 ml of *n*-hexane (II). The reforming catalysts were used without pretreatment (III-VI). After the hydrotreatment of the model compound and wood-based PO (I,II), the catalysts were washed in xylene and dried overnight at 100 °C. After the ATR of liquid HC and ethanol the reactor was flushed with nitrogen and then cooled down (III-VI).

The total amounts of carbon deposited on the noble metal catalysts after hydrotreatment of GUA and ATR, and the sulfur contents of the fresh and used Al₂O₃-supported CoMo catalyst were determined with a Leco SC-444 Carbon Sulfur analyzer (I,III-VI). Temperature programmed oxidation (TPO) and Raman spectroscopy were utilized to characterize the carbon deposits on the catalyst after the upgrading of PO (II). TPO experiments were carried out in a quartz reactor and the temperature was increased from room temperature to 700 °C (5 °C/min). Product gas was analyzed by Fourier transform infrared spectroscopy (FT-IR). Integration of the carbon monoxide and carbon dioxide peaks obtained as a function of time was used to estimate the amount of carbon deposited on the catalysts.

6.2 Catalyst testing

6.2.1 Hydrotreatment of guaiacol

Testing of the catalysts was performed in batch reactors. A solution of GUA in *n*-hexadecane was used as model compound for the lignin fraction of wood-based PO. After the pretreatment of the catalyst, 10 g of the solution was charged into the reactor. The pressure in the reactor was increased with hydrogen to 6 MPa or 4 MPa and the temperature was increased to 100 °C or 300 °C, respectively. The reaction pressure for both temperatures was 8 MPa, and this pressure was reached after the heating period. The reaction time was 1 - 4 h. (I)

Gas and liquid samples were taken only at the end of the experiment. Gas samples were analyzed by gas chromatography (GC), utilizing a thermal conductivity detector (TCD) and identification of compounds in the liquid samples was performed by gas chromatography/mass spectrometry (GC/MS). Quantification was performed by GC, utilizing a flame ionization detector (FID). The experiments and analysis of liquid and gas samples are described in more detail in I.

The conversions of GUA and the product distributions were calculated from the analyzed gas and liquid phases. The conversion of GUA (X_{GUA} (%)) was calculated from the initial

and final amounts (mol) of GUA (Eq. 34). Unreacted GUA was not included in the calculation of product distribution (P_i (mol%)) (Eq. 35). In Eqs. 34 and 35, $n(\text{product})_i$ represents moles of product.

$$X_{GUA}(\%) = \frac{n(GUA)_{initial} - n(GUA)_{final}}{n(GUA)_{initial}} \cdot 100\% \quad (34)$$

$$P_i = \frac{n(\text{product})_i}{\sum_{i=j}^m n(\text{product})_i} \cdot 100\% \quad (35)$$

After the hydrotreatment reaction, the oxygen to carbon (O/C) atomic ratio of the liquid product mixture should, due to the elimination of oxygen, be lower than the O/C atomic ratio of the reactant and the hydrogen to carbon (H/C) ratio should be higher, since hydrogenation is expected to take place. Thus, the O/C and H/C atomic ratios (Eqs. 36 and 37, n_i represents the number of atoms) of the liquid product mixture were used to estimate the success of the hydrotreatment. In these experiments involving the model compound, the composition of the product mixture based on GC quantification was used.

$$O/C(\text{atom/atom}) = \frac{\sum_{i=1}^m n(\text{oxygen})_{unreactedGUA \text{ and products}}}{\sum_{i=1}^m n(\text{carbon})_{unreactedGUA \text{ and products}}} \quad (36)$$

$$H/C(\text{atom/atom}) = \frac{\sum_{i=1}^n n(\text{hydrogen})_{unreactedGUA \text{ and products}}}{\sum_{i=1}^n n(\text{carbon})_{unreactedGUA \text{ and products}}} \quad (37)$$

6.2.2 Hydrotreatment of wood-based pyrolysis oils

The upgrading of wood-based PO was performed in a batch reactor at 20 MPa and 350 °C (II). The pinewood PO studied was provided by Technical Research Center of Finland (VTT, Espoo, Finland). The elemental composition of the PO used is presented in Table 4. Different analytical methods have been developed by VTT to identify and quantify the

chemical compounds in PO. Table 5 presents the chemical composition of a pinewood PO like the one used in II [112]. The results reported were obtained by the combination of solvent extraction and GC/MS. The quantification of all the components present in the sugar and lignin fractions is not possible with GC.

Table 4. Composition of pinewood PO. (II)

	Amount (wt-%)
C (wb)	40.1
H (wb)	7.6
N (wb)	0.1
S (wb)	0.01
O (by difference, wb)	52.1
O (db)	40.1
Water content	23.9
O/C molar ratio (db)	0.56
H/C molar ratio (db)	1.47

wb = wet basis, db = dry basis.

Table 5. Chemical composition of pinewood PO, combined results of solvent fractionation and GC/MS. [112]

Pyrolysis oil dry composition	Amount (wt-%)
Acid	5.6
Formic acid	1.5
Acetic acid	3.4
Propionic acid	0.2
Gycolic acid	0.6
Alcohols	2.9
Ethylene glycol	0.3
Methanol	2.6
Aldehydes, ketones, furans, pyrans	20.3
Non-aromatic aldehydes	9.7
Aromatic aldehydes	0.009
Non-aromatic ketones	5.36
Furans	3.37
Pyrans	1.10
Sugars	45.3
1,5-Anhydro- β -Darabino-furanose	0.27
Anhydro- β -D-glucopyranose	4.01
1,4:3,6-Dianhydro- α -D-glucopyranose	0.17
Hydroxy, sugar acids	
LMM lignin	17.7
Catechols	0.06
Lignin derivated phenols	0.09
Guaiacols (methoxy phenols)	3.82
HMM lignin	2.6
Extractives	5.7

db = dry basis, LMM= dichloromethane soluble lower-molecular mass fraction of water-insoluble, HMM= dichloromethane insoluble higher-molecular mass fraction of water insoluble

After the pretreatment of the catalyst (noble metal catalysts and sulfided CoMo/Al₂O₃), 25 ml of wood-based PO were introduced to the reactor at room temperature. The reactor was then flushed with hydrogen and the pressure increased to 8 MPa hydrogen. The temperature of the reactor was then increased to 350 °C and a reaction pressure of 20

MPa was reached. During the reaction time (1-4 h) hydrogen was not added to the reactor and no sampling was performed. After the reaction the reactor was cooled down and opened. The gas and liquid phases were collected and analyzed. The liquid phase was centrifuged to separate the organic, water, and solid phases. The gas phase was analyzed with GC, utilizing a TCD. The water content of the organic phase was measured using a Karl Fischer titration device (Metrohm 702 SM Titrino). The elemental composition (O, H, and C) of the organic and aqueous phases was measured with a EuroVector EA3400 Series CHNS-O analyzer with acetanilide as reference. The oil phase was also characterized by ^1H - and ^{13}C - nuclear magnetic resonance (NMR, Varian AS400 spectrometer) using CDCl_3 as solvent. Gel permeation chromatography (GPC) was performed using a high performance liquid chromatography analyzer (HPLC, Agilent 1200) equipped with a refractive index detector. Polystyrene was used as calibration standard. The thermal stability of the organic phase was studied by thermo-gravimetric analyses (TGA, Perkin-Elmer). Inductively coupled plasma – optical emission spectrometry (ICP-OES) analysis of the aqueous product phase was performed using an Optima 700 DV (Perkin Elmer) analyzer. Inductively coupled plasma – mass spectrometry (ICP-MS) was utilized to measure the metals in the aqueous product phase. The presence of metal in this phase indicates the leaching of metals from the catalyst. Capillary electrophoresis (CE, Agilent Technologies) was used to determine the amount of organic acids in the aqueous phase after reaction. (II)

In hydrotreatment reactions, hydrogen consumption (hydrogen uptake) during the reaction is of major interest and was calculated as follows

$$n_{\text{H}_2, \text{initial}} = \frac{V_{\text{gas cap}} \cdot P_{\text{initial}}}{R \cdot T_{\text{initial}}}, \quad (38)$$

where $n_{\text{H}_2, \text{initial}}$ is the initial amount of hydrogen (in moles) in the reactor, $V_{\text{gas cap}}$ is the volume of the gas phase, P_{initial} is the initial pressure in the reactor (at room temperature), R is gas constant, and T_{initial} is the initial temperature in the reactor (at room temperature).

After the reaction, the reactor was cooled to room temperature and the total pressure was recorded. The amount of hydrogen at the end of the reaction is given by

$$n_{\text{H}_2, \text{final}} = y_{\text{H}_2, \text{final}} \frac{V_{\text{gas cap}} \cdot P_{\text{final}}}{R \cdot T_{\text{final}}}, \quad (39)$$

where $n_{\text{H}_2, \text{final}}$ is the amount of hydrogen (in moles) in the reactor after the reaction, $y_{\text{H}_2, \text{final}}$ is the mol fraction of the hydrogen in the gas phase (gas cap) after the reaction (as measured

by GC-TCD), P_{final} is the pressure in the reactor after the reaction (measured at room temperature) and T_{final} is the final temperature in the reactor (at room temperature).

With this information, hydrogen uptake per kg feed was calculated using Eq. 40.

$$H_2 uptake = \frac{\left(n_{H_2, initial} - n_{H_2, final} \right) \cdot \frac{R \cdot 298K}{1 \text{ atm}}}{m_{PO, initial}}, \quad (40)$$

where $H_2 uptake$ is the hydrogen consumption (in normal liters, NL) per kg feed and $m_{PO, initial}$ the initial mass of wood-based PO.

In paper II the activity of the catalysts was calculated taking into consideration the total amount of metal in the catalyst. However, owing to the completely different amounts of metals on the catalysts in this summary, the activity based on the mass (g) of catalyst is preferred in the comparison of the catalysts (Catalyst activity*, Eq. 41). The activity of the catalyst is calculated from the hydrogen consumption (Eq. 40), catalyst amount (Eq. 41) or metal loading of the catalysts (mass of metal assuming that all the metal is active, Eq. 42), and reaction time (h).

$$Catalyst \ activity^* \left(\frac{NL_{Hydrogen}}{kg_{PO} \cdot g_{cat} \cdot h} \right) = \frac{H_2 uptake}{m_{catalyst} \cdot h} \quad (41)$$

$$Catalyst \ activity \left(\frac{NL_{Hydrogen}}{kg_{PO} \cdot g_{metal} \cdot h} \right) = \frac{H_2 uptake}{m_{metal} \cdot h} \quad (42)$$

6.2.3 Autothermal reforming of simulated and conventional fuels

Screening and testing of the noble metal catalysts was performed in a continuous tubular quartz reactor. The reactor was packed with the catalyst, placed in the furnace and a thermocouple was placed inside the catalyst bed to monitor the temperature inside the reactor. The feed compounds, water, HC, and gases (air and argon) were evaporated and mixed prior to the reactor. The feed and products were analyzed online with a FT-IR. The flows were diluted with nitrogen prior to the analyzer. More details concerning the experimental procedures are given in III-VI.

n-Heptane (H) and *n*-dodecane (D) were used as model compounds for the *n*-alkane fractions of gasoline and diesel, respectively, and toluene (T) and methylcyclohexane (MCH) as model compounds for the aromatic and cycloalkane fractions. A mixture of MCH/H/T = 50/30/20 (mol%) was used to simulate gasoline and a mixture of 80 mol% D, and 20 mol% T was used to simulate diesel. Experiments with simulated gasoline and diesel were performed with (IV) and without (III,V) the addition of a sulfur-containing compound (4,6-dimethyldibenzothiophene, 4,6-DMDBT). ATR of commercial diesel (NExBTL, Neste Oil, IV) was studied in the same system. The performance of the catalysts was also tested in the ATR of ethanol (VI). The steam to carbon (H_2O/C) and the oxygen to carbon (O_2/C) molar ratios of the feeds were estimated based on the thermodynamic study of the systems and these values were used in the calculation of the liquid flow to the reactor (III-VI).

The feed and product flow were diluted with nitrogen (900 cm³/min normal temperature and pressure, NTP) and analyzed with an on-line FT-IR spectrometer (Gasmét™) equipped with a Peltier-cooled mercury-cadmium-telluride (MCT) detector and multicomponent analysis software (Calcmét). The sample cell was kept at 230 °C to avoid condensation of the HC and the water. The compounds analyzed by FT-IR were water, carbon monoxide, carbon dioxide, methane, C₂H₂, C₂-C₅ alkenes, C₂-C₇ alkanes, C₁-C₄ alcohols, benzene, T, cyclohexane, and MCH.

The conversions of HC and water were calculated from the feed and product flows (F_i , mol/min, Eq. 43). The weight average conversion (X_i) of HC was calculated to determine the overall hydrocarbon conversion (X_{tot} , Eq. 44).

$$X_i = \frac{F_{i,in} - F_{i,out}}{F_{i,in}} \cdot 100\% \quad (43)$$

$$X_{tot} = \sum_{i=1}^m (n_{i,in} \cdot X_i) \quad (44)$$

The amounts of oxygen consumed, hydrogen produced and the balances of elements were calculated using the analyzed product distribution and the measured dry gas flow. P_i and the yield (Y_i , mol/mol C_{in} , C_{in} is the carbon in the feed) were calculated according to Eqs. 45 and 46, respectively.

$$P_i = \frac{F_i}{\sum_{n=1}^j F_n} \cdot 100\% \quad (45)$$

$$Y_i = \frac{F_i}{F_{C_{in}}} \quad (46)$$

Hydrogen is formed in reforming reactions and in the equilibrium WGS reaction. Therefore, the hydrogen production does not reveal the affinity of the catalyst only for reforming reactions. The selectivity of the catalysts for reforming reactions was presented as the reforming to oxidation molar ratio (*Ref/Ox*, Eq. 47). In the *Ref/Ox* molar ratio, the effect of the WGS reaction was eliminated.

$$Ref/Ox = \frac{P_{H_2} + P_{CO}}{P_{H_2O} + P_{CO_2}} \quad (47)$$

In the ATR of ethanol the yield of desired products ($Y_{desired\ products}$) was calculated (Eq. 48) where F_{H_2} , F_{CO} , and F_{CH_4} are the molar flows of hydrogen, carbon monoxide, and methane in the outlet of the reactor.

$$Y_{desired\ products} (mol/mol) = \frac{F_{H_2} + F_{CO} + F_{CH_4}}{F_{EtOH, in}} \quad (48)$$

The carbon present in ethanol is converted into desired carbon containing products (carbon monoxide and methane) and undesired carbon dioxide. The ratio of desired to undesired carbon products is expressed by Eq. 49.

$$Desired\ to\ undesired\ carbon\ products (mol/mol) = \frac{F_{CO} + F_{CH_4}}{F_{CO_2}} \quad (49)$$

7 Hydrotreatment

7.1 Guaiacol as model compound

GUA was studied as model compound for the lignin fraction of wood-based PO. ZrO₂-supported noble metal catalysts and a commercial sulfided CoMo/Al₂O₃ catalyst were tested in the reactions of GUA in the presence of hydrogen at different temperatures (I).

7.1.1 Thermodynamics

When an oxygen-containing molecule is hydrotreated, HDO takes place. Often HDO is understood as oxygen removal from a chemical compound in the form of water. This requires a catalyst together with high hydrogen pressures and temperatures. The oxygen removal does not, however, happen in one step, as indicated in Figure 4. In the presence of hydrogen and catalyst, GUA undergoes several reactions involving oxygen-containing aromatic compounds, oxygen-free substituted aromatics, saturated oxygen-containing compounds, and partially saturated compounds. As simplified examples of the reactions taking place during HDO the following four stoichiometric reactions (Eqs. 50-53) were selected for thermodynamic evaluation based on products detected in the liquid and gas phases.



The thermodynamic calculations (HSC [113]) were performed for the gas phase system at atmospheric pressure and the results are presented in Figure 6. According to the thermodynamic calculations, reactions yielding hydrogenated products are more favorable in the temperature range below 270 °C while at temperatures above 270 °C, reactions giving oxygen-free aromatic products prevail.

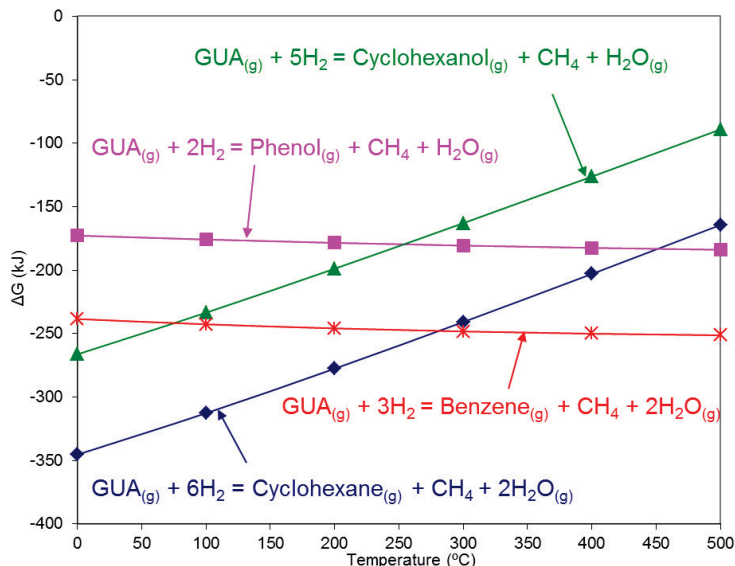


Figure 6. Thermodynamic calculation for possible reactions in the hydrotreatment of GUA [113].

7.1.2 Effect of temperature on the reactivity of guaiacol

The model compound was tested in the batch reactor at 8 MPa at 100 °C and 300 °C. After the reaction, the liquid and gaseous products were analyzed. The conversions and product distributions achieved in the catalytic tests are presented in Figure 7. Temperature had a significant effect on the reactions of GUA. At 100 °C complete conversion of GUA was achieved only with Rh and RhPt, while at 300 °C conversions higher than 70% were reached with all catalysts. (I)

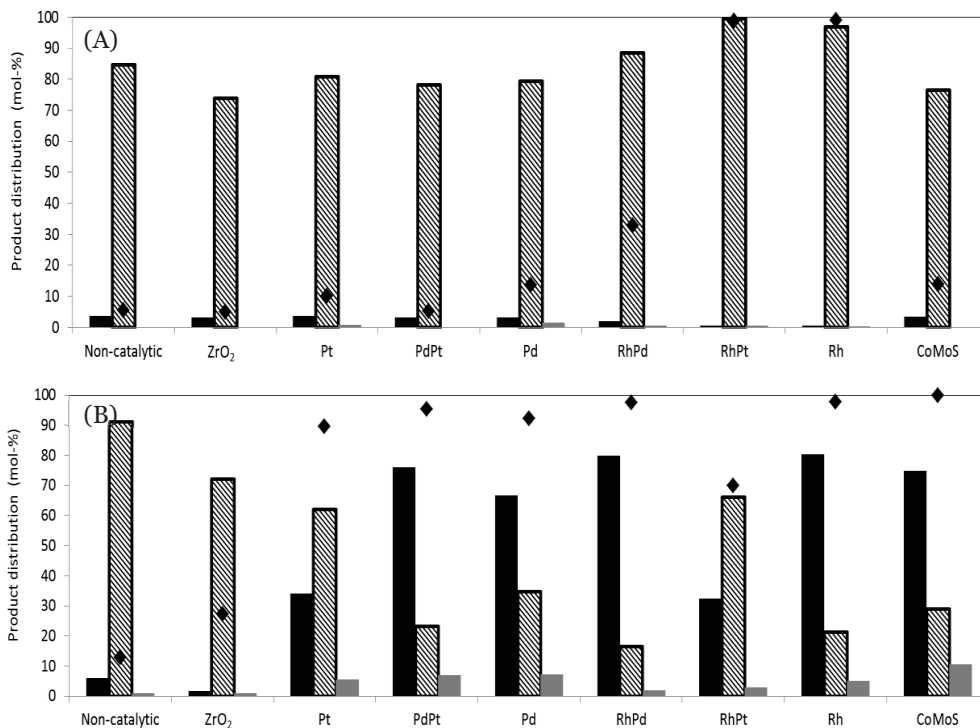


Figure 7. Conversion and product distribution at 100 °C and 300 °C without catalyst, with ZrO₂ support, and with ZrO₂-supported noble metal and sulfided CoMo/Al₂O₃ catalysts. A) T= 100 °C and B) T= 300 °C. ♦ Guaiacol conversion, ■ oxygen-free products (hydrogenated or non-hydrogenated), and ▨ hydrogenated products (oxygen-containing or oxygen-free).

At 100 °C all the noble metal catalysts were found to be selective towards hydrogenated oxygen-containing compounds. The main component of the product mixture was 1-methyl-1,2-cyclohexanediol. Also methoxycyclohexanol, methoxycyclohexanone, and methoxycyclohexane were identified. (I)

The performance of the Rh catalyst was studied as a function of time and the results are presented in Figure 8. As shown in this figure, at 100 °C and short reaction times the main product was 1-methyl-1,2-cyclohexanediol. Its concentration increased in the two first hours but after that started slowly to decrease. Also 1,2-dimethoxybenzene, cyclohexanol, and 2-methoxycyclohexanone were detected but their concentrations decreased continuously indicating that they are reaction intermediates. After three hours the production of 1,2-dimethoxycyclohexane started. In addition minor quantities of cyclohexane were found during the whole test. (I)

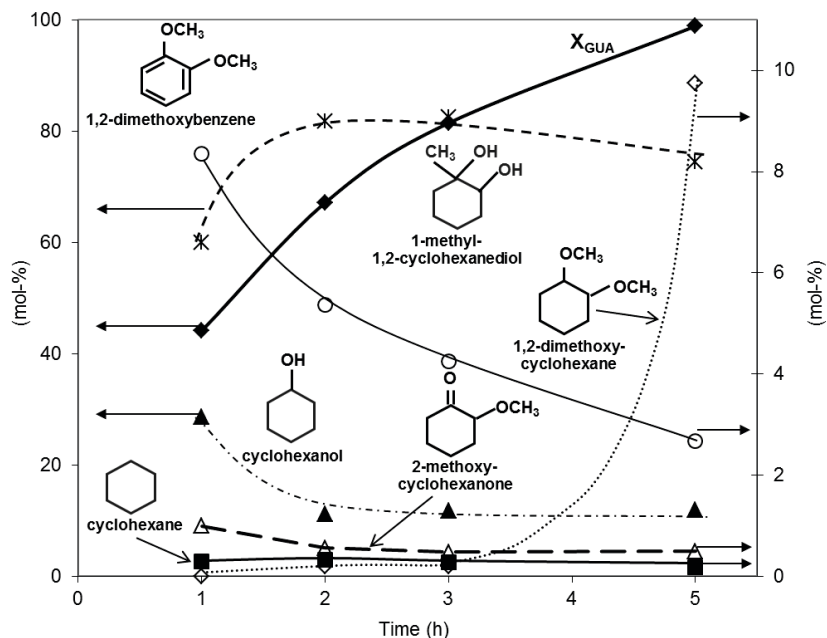


Figure 8. Guaiacol conversion and distribution of main products for experiments with R/ZrO₂ at 100 °C, 8 MPa and 1-5 h. (I)

At 300 °C, Pd, PdPt, RhPd, and Rh catalysts were selective towards deoxygenated compounds (oxygen-free compounds, Figure 7, B), with benzene or methyl-substituted benzenes being the main liquid products meaning that ring saturation was remarkably less than at 100 °C. The Pt catalyst produced more hydrogenated products than deoxygenated ones. Similar behavior was detected for the RhPt although Rh exhibited high deoxygenation activity at the same conditions. (I)

Because of the high conversions of GUA at 300 °C, the catalysts can be compared based on product distribution. The van Krevelen diagram [114] is typically used to assess the origin and maturity of petroleum. The diagram presents the H/C as a function of O/C atomic ratios of a compound. It is desired that after the hydrotreatment, the H/C and O/C atomic ratios of the reaction mixture are close to those of gasoline and diesel ($H/C= 1.8-2$ atom/atom, $O/C= 0-0.002$ atom/atom [115]).

The van Krevelen diagram for the different product mixtures (unreacted GUA and products) is shown in Figure 9. The Rh/ZrO₂ catalysts resulted in the highest oxygen removal with less hydrogenation and therefore less hydrogen consumption than the other catalysts tested. H/C atomic ratios close to 1 indicate the aromatic nature of the product (benzene). (I)

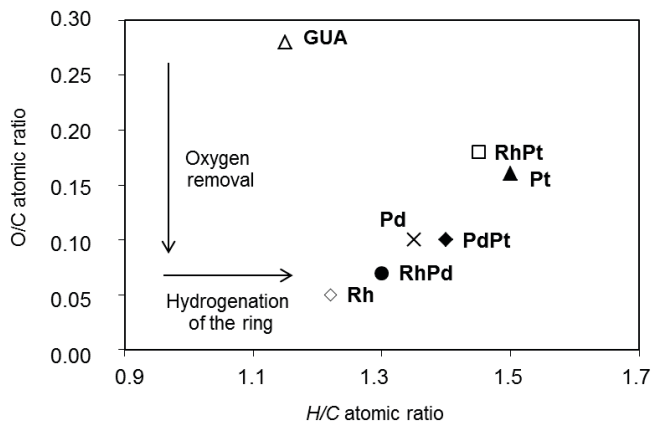


Figure 9. van Krevelen diagram for HDO of guaiacol with noble metal catalysts (300 °C, 8 MPa, 4 h). The ratios are calculated for the reaction mixture (unreacted guaiacol and liquid products). (I)

In the presence of hydrogen, GUA underwent a set of consecutive and parallel reactions. According to calculations the hydrogenation of GUA and the formation of oxygen-free products were not limited by thermodynamics [113]. At high temperatures hydrogen availability in the reaction mixture was the highest (I), yet yielding aromatic products. Ring saturation did not dominate at high temperatures, but was clearly present at low temperatures. The hydrogen equilibrium coverage of the catalyst surface decreased with temperature, as adsorption is an exothermic reaction [116,117]. This was not expected to influence the rate of hydrogenation and hydrodeoxygenation reactions because there was excess hydrogen in the liquid phase. Even though at low temperatures hydrogen solubility was lower than at high temperatures (I), the formation of saturated products indicated that there was lack of hydrogen neither.

7.1.3 Carbon deposition

The amount of carbon deposited on the catalysts at 100 °C and 300° C is shown in Table 6. Independently of the reaction temperature, less deposition of carbon was measured on the noble metal catalysts than on the commercial sulfided Al₂O₃-supported CoMo. Furthermore, methane and light HC were detected in the gas phase of experiments performed with the noble metal catalysts. Carbon monoxide and carbon dioxide, the respective products of decarbonylation and DCO, were not detected although their

presence was expected in the gas phase. The low deposition of carbon on the noble metal catalysts could result from their activity in carbon gasification reactions [118] and the affinity of these catalysts for the reactions of carbon monoxide, carbon dioxide, and hydrogen that yield methane, the main product of the gas phase. Hossain [119] proposed that the spillover mechanism exhibited by noble metals catalysts to donate hydrogen is the reason for the low carbon deposition. Hydrogen spillover influences the cracking reaction by controlling the concentration of carbonium ions and other unstable reaction intermediates. Thus, the deposition of carbons or HC was prevented by converting them into stable products.

Table 6. Carbon deposits on ZrO₂-supported mono- and bimetallic noble metal catalysts and sulfided CoMo/Al₂O₃ after guaiacol hydrotreatment tests at 100 °C and 300 °C at 8 MPa. (I)

Carbonaceous deposits (wt-%)	ZrO ₂	Pt	PdPt	Pd	RhPd	RhPt	Rh	CoMo/Al ₂ O ₃ (sulfided)
100 °C	0.5	0.6	0.4	0.6	1.0	1.0	1.8	6.7
300 °C	2.0	2.6	0.6	2.6	0.6	1.7	0.6	9.7

7.2 Wood-based pyrolysis oil

The noble metal catalysts were also tested in the upgrading of wood-based PO. For comparative purposes, the upgrading was also performed with sulfided CoMo under the same conditions.

The experiments with the noble metal catalysts yielded fewer components to the gas phase than the sulfided CoMo. The gaseous product consisted of a mixture of unreacted hydrogen (~80 wt-%), the concentrations of carbon dioxide, light HC, and carbon monoxide varied depending on the catalyst used. Less carbon dioxide and carbon monoxide, and more methane were, however, produced with the noble metal catalysts than with the sulfided CoMo. (II)

Two immiscible liquid phases were obtained, a dark brown bottom organic phase (37-47 wt-%, containing, e.g., ketones, lignin-derived phenols, methoxyphenols, cyclopentane, cyclohexene, and cyclohexane) and a yellowish top aqueous phase (28-36 wt-%, mainly containing acetic acid, and methanol). Some solids (char, 1.5-15 wt-% of feed) were also formed. (II)

7.2.1 Catalyst screening

The catalyst activity calculated on the basis of hydrogen consumption and the total mass of catalysts (Eq. 41) for the different catalysts tested is presented in Figure 10.

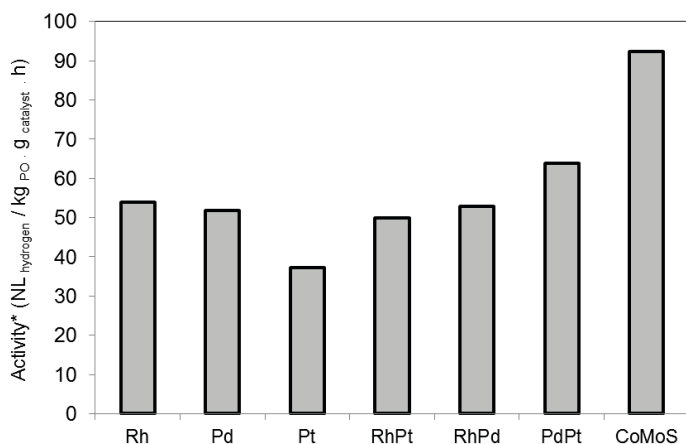


Figure 10. Catalyst activity (Catalyst activity*, Eq. 41) for the mono- and bimetallic catalysts tested for hydrotreatment of PO at 350 °C and 20 MPa total pressure for 4 h. (II)

The noble metal catalysts were active in the upgrading of wood-based PO. The least active one was the monometallic Pt catalyst, the most active being sulfided CoMo. A similar activity level was achieved with the Rh-containing and monometallic Pd-catalysts. Addition of Pd to Pt improved clearly the activity of the Pt. (II)

Figure 11 presents the oxygen content of the organic phase (on a dry basis) based on elemental analysis. The oxygen content of the upgraded wood-based PO was significantly lower than that of the original material. However, there was no major difference between the catalysts, and similar oxygen content was also achieved with the conventional sulfided CoMo.

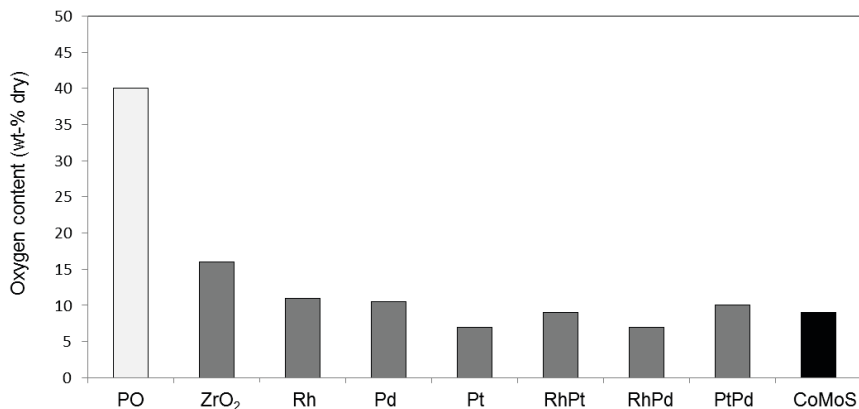


Figure 11. Oxygen content of pyrolysis oil (PO) and hydrotreated oils (350 °C, 20 MPa and 4 h).

The van Krevelen diagram for the organic liquid phase (on a dry basis) is presented in Figure 12. The *O/C* atomic ratio was similar with all catalysts. Differences were, however, detected in the *H/C* atomic ratio. Because the *O/C* ratios for the catalytic and non-catalytic experiment were similar, the decrease in the oxygen content was likely due to thermal polymerization reactions, in which oxygen was also removed in the form of water instead of resulting from catalytic HDO reactions. Therefore, the *H/C* atomic ratio was here a more suitable measure of the hydrogenation/hydrodeoxygenation activity of the catalyst. Upgraded wood-based POs with 1% oxygen content has been reported by Elliot et al. [62], Elliot and Schiefelbein [120], and Elliot and Oasmaa [121] using sulfided CoMo and NiMo catalysts. However, the process involves 2 steps. In the first one, taking place at a low temperature (270 °C and 14 MPa) thermally unstable compounds that would otherwise coke and plug the reactor, were hydrotreated. In the second step, hydrogenation at high temperature took place (400 °C and 14 MPa). The oil produced had a research octane number of 72, and an aromatic/aliphatic carbon ratio of 0.28-0.56.

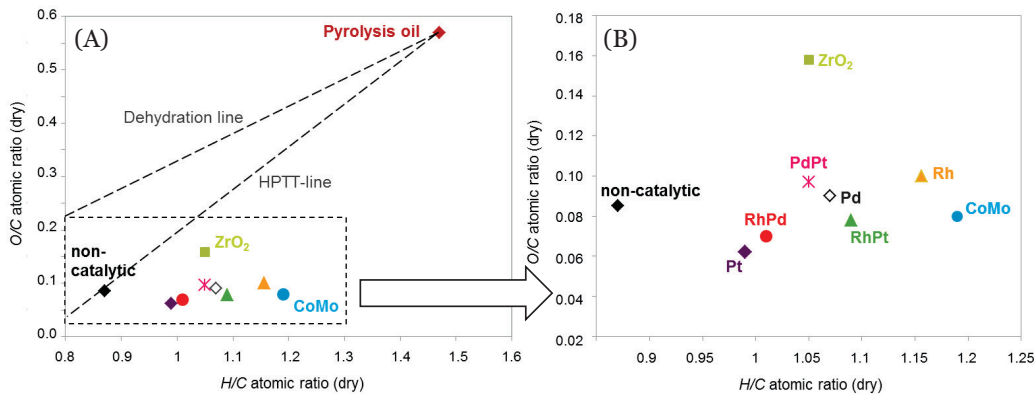


Figure 12. van Krevelen diagram for the hydrotreated oils with noble metal catalysts. HPTT-line= thermal removal (drying) of oxygen. (II)

Figure 13 shows the activity of the catalysts (Eq. 41) as a function of the $H/C - H/C_{thermal}$ atomic ratios. In the $H/C - (H/C)_{thermal}$ ratio ($(H/C)_{thermal}$ = atomic ratio for the non-catalytic tests), the contribution of thermal hydrogenation reactions was eliminated and only the effect of catalytic reaction was considered. The most active of the noble metal catalyst was PdPt. Rh, RhPt, Pd, and RhPd exhibit similar activities, the least active being Pt. The main difference was in the degree of hydrogenation level achieved with the catalysts. Rh was the most active one in hydrogenation, followed by RhPt, Pd, PdPt, and RhPd, the least active ones in hydrogenation reactions being RhPd and Pt. Sulfided CoMo possessed the highest hydrogenation activity.

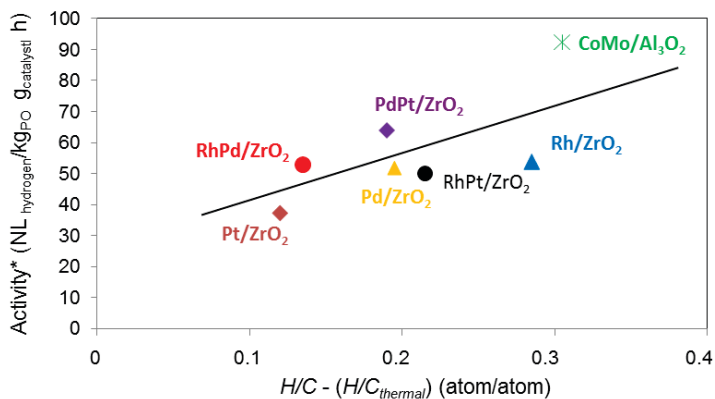


Figure 13. Activity of the catalysts as a function of $(H/C - (H/C)_{thermal})$ atomic ratio.

The liquid product was analyzed after the tests by using ^1H - and ^{13}C -NMR. These determinations revealed that the noble metal catalysts yielded a more aromatic product while the formation of alkanes was higher with the sulfided catalyst than with the noble metal ones, in agreement with the high hydrogen consumption calculated. (II)

The mass-average molecular weight (M_w) was measured by GPC, using polystyrene as reference. The M_w of the upgraded product was higher than of PO. Thus, polymerization reactions took place under the conditions tested. Thermal stability of the upgraded oil was measured by TGA, in which a small residue indicated a low coking tendency of the product. Smallest residue was found for the catalysts with the highest H/C atomic ratios or the highest hydrogen consumption (Rh and sulfided CoMo). The TGA residue was related to the M_w of the product and therefore to the hydrogen consumption. For catalysts with high hydrogen consumption, the product had usually a low M_w and, as a result, small TGA residue. (II)

7.2.2 Catalyst stability

Owing to the harsh conditions (high temperatures and pressures, presence of water and acids), stability of the catalyst is major concern in the upgrading of PO. As an example of catalyst stability, Figure 14 presents the changes in hydrogen consumption and activity as a function of time for the Rh catalyst. The hydrogen consumption leveled off after 4 h. The main reasons could be a decrease in the activity of the catalyst or that less reactive compounds predominated in the reaction mixture as the reaction proceeded. At short reaction times the M_w was high, but decreased considerably as the reaction time increased. Thus, thermal polymerization took place in the beginning of the reaction and only after this period the large M_w molecules depolymerized, most likely through hydrogenation. (II)

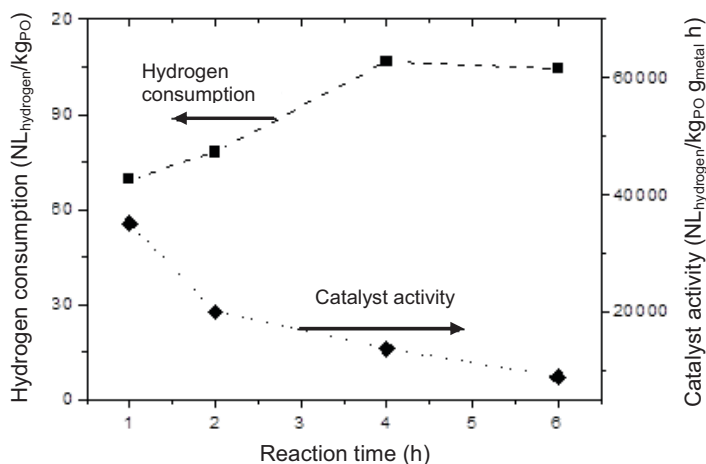


Figure 14. Hydrogen consumption and catalyst activity as a function of time for hydrogenation of PO with Rh/ZrO₂ (350 °C 20 MPa total pressure). (II)

Leaching of active metals and the support could take place under the conditions used, reducing the activity and time-on-stream of the catalysts. ICP-OES was used to measure the leaching of metals and support. ICP-OES performed on the aqueous product from tests with noble metal catalysts revealed no detectable amounts of metals. However, Co and Al were detected in the aqueous phase of tests performed with sulfided CoMo indicating that it was not stable under the hydrogenation conditions used. (II)

Carbon deposited on the catalysts during the hydrotreatment of PO. The used noble metal catalysts were studied by TPO to quantify this deposits (quantification based on the amounts carbon dioxide and carbon monoxide formed) and also to identify a suitable temperature to ensure complete burning of the carbon deposits. Raman spectroscopy was used to determine the nature of the carbon deposits.

The carbon deposited on the noble metal catalysts was 2-3 wt-% and for the sulfided CoMo was 5 wt-%. The highest deposition was measured on plain ZrO₂ (7 wt-%). The slightly acidic nature of ZrO₂ [100] catalyzed the formation of carbon deposits. Since ZrO₂ was not active in hydrogenation reactions (low hydrogen consumption, see Figure 12), the dominant path was polymerization leading to high-molecular-weight products and carbon deposition. (II)

The carbondioxide thermograms from the TPO measurements for the used noble metal catalysts exhibited a broad peak with a maximum at 360-370 °C only differing in intensity between catalysts. Higher temperatures were required to burn the carbon deposits on

sulfided CoMo, probably owing to the lower activity of this catalyst in gasification reactions. (II)

The Raman spectra of fresh and used Rh and the catalyst after TPO are presented in Figure 15. Because of the low metal loading (max. 0.5 wt-%) used, no difference could be observed between the ZrO_2 support and the fresh catalysts. The Raman spectrum contained only two peaks for the used noble metal catalysts. These peaks corresponded to polycrystalline and imperfect graphite (1350 cm^{-1}) and graphite coke (1580 cm^{-1}) [122]. The Raman spectrum of the catalyst after the TPO analysis revealed the original structure of the noble metal catalyst. Similar results were obtained with all the other noble metal catalysts.

After the TPO of sulfided CoMo, Raman spectrum still exhibited the peaks for the polycrystalline and imperfect graphite (not shown). Burning of the carbon deposits was thus not complete, as observed for the noble metal catalysts.

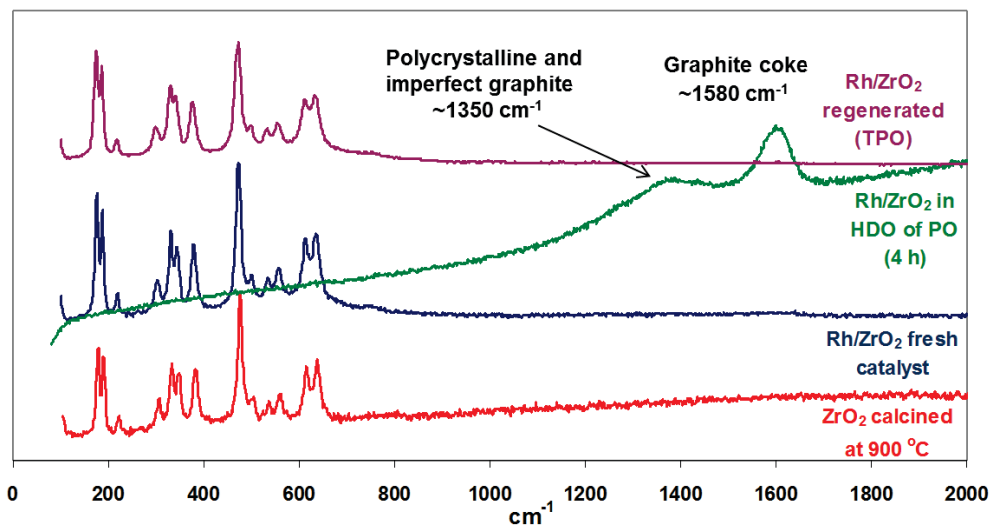


Figure 15. Raman spectra for ZrO_2 , fresh, used (in hydrtreatment of pyrolysis oil (PO)), and after TPO Rh/ZrO₂ catalyst. (II)

8 Autothermal reforming

ZrO₂-supported mono- and bimetallic Rh and Pt catalysts were tested in the ATR of simulated gasoline (III,V) and diesel (IV), commercial diesel (IV), and ethanol (VI). The ability of these catalysts to tolerate low concentrations of sulfur was also studied (IV). The presence of sulfur-containing compounds in the feed was simulated with 4,6-DMDBT and hydrogen sulfide. 4,6-DMDBT is a compound that is difficult to remove in the HDS processes. This is due to the steric hindrance of the methyl groups that prevents the contact between the sulfur-containing group and the active site of the catalyst [123,124]. For this reason, 4,6-DMDBT is found in low-sulfur diesel fuel. Hydrogen sulfide is often used as model compound for sulfur-containing compounds.

In ATR the catalysts were used without any pretreatment because in preliminary studies hydrogen pretreatment had only a negligible effect on the performance of catalysts. Studies on the ATR of HC also revealed that the active site in the Rh-containing catalysts was the oxide Rh₂O₃ [125], and thus, any pre-reduction of these ATR catalysts was not required. (III)

8.1 Simulated gasoline and diesel

Mono- and bimetallic Rh- and Pt-containing catalysts were tested in the production of hydrogen and hydrogen-rich mixtures from simulated gasoline (heptane/toluene/methylcyclohexane (H/T/MCH) = 20/30/50, mol%, III) and diesel (dodecane/toluene (D/T) = 80/20, mol%, IV,V).

8.1.1 Catalyst screening

Complete conversion of the simulated gasoline and diesel was achieved with the noble metal catalysts tested at temperatures higher than 600-700 °C. At low temperatures the conversions achieved with the Rh- and Pt-containing bimetallic catalysts were between the values obtained with the monometallic catalyst. The conversion of oxygen was complete for all catalysts and temperatures tested, indicating the high activity of the noble metal catalysts in oxidation reactions (POx and Ox). (IV,V)

The product distribution achieved for the ATR of simulated gasoline on the different catalysts is presented in Table 7. The thermodynamic equilibrium of the products and the results obtained for ZrO₂ and from the non-catalytic experiments are also presented in the table for comparative purposes.

Table 7. Conversion (weighted average of hydrocarbons) and product distribution (mol%) in ATR of simulated gasoline (methylcyclohexane/heptane/toluene= 50/30/20, mol%) at the inlet temperature of 700 °C. All catalysts were calcined at 900 °C. (III)

	Conversion (mol%)		Distribution of products (mol%)					CO/CO ₂ (mol/mol)
	Simulated gasoline (average)	Water	H ₂	CO	CO ₂	CH ₄	Others	
Thermo-dynamics	100	2	67	11	23	0	0	0.5
No catalyst	47	4.8	61	9.0	0.2	4.9	25	45.0
ZrO ₂	51	-5.7	27	53	14	3.6	2.1	3.7
Pt	53	4.9	50	29	17	0.9	3.1	1.7
0.5RhPt	98	27	61	17	21	0.2	0.2	0.8
1RhPt	97	29	62	18	20	0.4	0.5	0.9
2RhPt	99	27	63	17	19	0.3	0.2	0.9
Rh	97	29	59	17	22	0.3	0.6	0.8

A similar conversion level was reached in the non-catalytic tests and in the tests performed with ZrO₂. However, ZrO₂ yielded higher amounts of CO_x and lower amounts of hydrogen than the non-catalytic experiment together with water formation as indicated by the negative value for the water conversion. Therefore, it could be concluded that ZrO₂ exhibit some activity in oxygenation reactions (POx and Ox), resulting in CO_x and water as main products. (III)

The product distribution on the Rh-containing catalyst was close to thermodynamic equilibrium. Furthermore, low concentrations of light HC (C₂-C₃-HC designated as

“others” in Table 7) and methane were measured for these catalysts, indicating a high selectivity of the Rh-containing catalyst in reforming reactions. (III)

The selectivity of the catalysts towards reforming reactions was presented in the reforming to oxidation molar ratio (Ref/Ox , Eq. 47). In this ratio the effect of the WGS reaction was eliminated. Figure 16 shows the effect of metal loading on the Ref/Ox (Eq. 47) and on carbon deposition. The addition of low amounts of Rh improved the performance of the bimetallic catalyst over that of the monometallic Pt. Catalysts with different Rh/Pt ratios yielded similar HC conversions and thus, this metal ratio had a limited effect on the total activity of the bimetallic catalysts. However, catalysts with a higher Rh concentration exhibited higher Ref/Ox molar ratio than the catalyst with more Pt, owing to the high activity of Rh towards reforming reactions. This was also evident from the low formation of carbon deposits measured for the catalysts with high Rh content. Furthermore, the deposition of carbon on the bimetallic catalysts calcined at 700 °C was lower than on the monometallic catalysts calcined at the same temperature. (III)

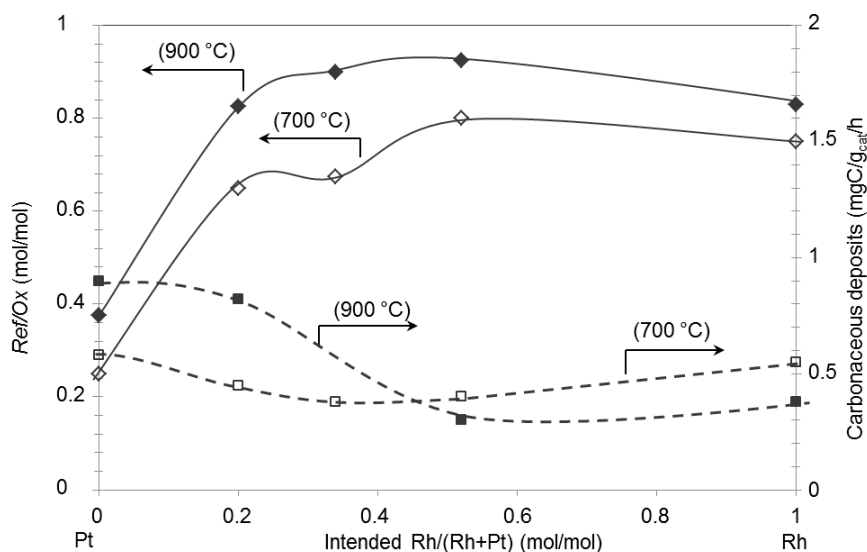


Figure 16. Effect of Rh/(Rh+Pt) molar ratio on the Ref/Ox ratio (◆) (mol/mol) of the products and on the average carbon deposition (■) (mgC/g_{cat}/h) in ATR of simulated gasoline on mono- and bimetallic RhPt catalysts (0.2 g) calcined at 700 °C (open symbol) and 900 °C (filled symbol). $H_2O/C=3$ mol/mol, 700 °C for 5 – 6 h. (III)

Carbon deposits formed and removed from the surface of the catalysts, whereby a steady state with regard to the amount of carbon was reached on the catalyst. The average amounts of carbon formation shown in Figure 16 was in agreement with the values (0.8–0.9 mg carbon/g_{cat}/h) reported by Souza and Schmal [126] for Pt/ZrO₂ catalysts tested in the dry reforming of methane. The carbon monoxide to carbon dioxide (CO/CO_2) molar

ration presented in Table 7 for Pt was higher than that observed for the other catalysts (Table 7, III). This indicated that reverse Boudouard reaction (Eq. 29) was the main reaction involved in the gasification of carbon. The high CO/CO_2 molar ratio calculated for ZrO_2 could be explained by the ability of ZrO_2 to release oxygen, promoting the formation of carbon monoxide [127].

8.1.2 Catalyst stability

In short stability tests (6 h) the decrease in the hydrocarbon conversion and the increase in thermal cracking products were clear indications of deactivation of the Rh catalyst calcined at 700 °C. The addition of Pt improved the stability of the Rh-catalysts as no decrease in the conversion was detected and the concentration of thermal cracking products did not increase with the Rh-containing bimetallic catalysts.

The calcination temperature of the catalyst seemed to have a stabilizing effect on the surface. The concentration and product distribution achieved with the catalysts calcined at 900 °C remained constant during the short stability tests. It has been proposed that the activity of Rh is directly proportional to the availability of Rh while in the case of Pt the activity is directly proportional to the Pt- ZrO_2 interface [127]. Thus, the Rh catalyst was more sensitive to deactivation than the Pt- and bimetallic catalysts.

8.2 Ethanol

Mono- and bimetallic Rh- and Pt-containing catalysts were tested in the ATR of ethanol. The behavior of these catalysts was compared with that of the commercial NiO/Al_2O_3 catalyst.

8.2.1 Catalyst screening

The conversions of reactants and catalyst bed temperatures for the different catalysts tested are presented in Figure 17. Complete conversion of ethanol and oxygen was achieved on the commercial and Rh-containing catalysts. Water was formed in cases where the conversion of ethanol was incomplete. The endothermicity of the total reaction correlated with the water conversion, indicating strong STR activity for Rh-containing catalysts and the commercial NiO/Al₂O₃ catalyst. The high activity of Rh was in agreement with the work of Liguras et al. [128] who tested Rh, Ru, Pt, and Pd (metal loading 0-5 wt-%) in STR of ethanol within the temperature range of 600-850 °C, and reported Rh to be the most active noble metal catalyst at low Rh loads. ZrO₂ had a limited catalytic effect and thermal reactions predominated.

Based on product distribution with the Pt catalyst, thermal reactions were present at 700 °C and based on the conversion of oxygen achieved, some oxidation reactions were catalyzed. At low temperatures (300-450 °C), however, Pt catalysts have been reported [129] to be the most active ones in the STR of ethanol.

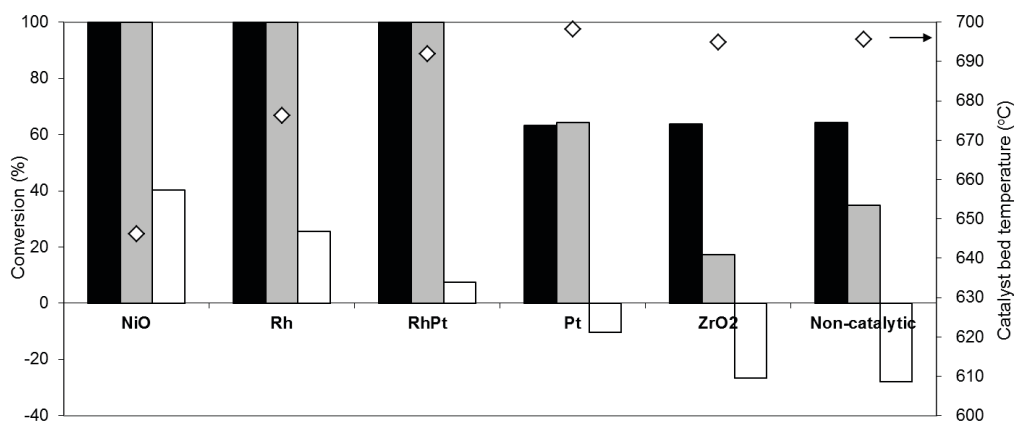


Figure 17. Conversion of ethanol (■), oxygen (■), water (□) in ATR at inlet temperature of 700 °C. ZrO₂ calcined at 900 °C (16 h), and catalysts calcined at 700 °C (1 h). Catalyst bed temperature (◊). Conditions: H₂O/C = 2 mol/mol, and O₂/C = 0.2 mol/mol, duration = 5 h. (VI)

The product distributions obtained with the different catalysts are presented in Figure 18. The calculated thermodynamic concentration for hydrogen [113] was reached with the Rh-containing catalysts, but was not achieved in experiments where the conversion of ethanol was incomplete. Results similar to those obtained in the experiment without any

catalyst, indicated in these cases light HC were produced via non-catalytic dehydration or cracking reactions. (VI)

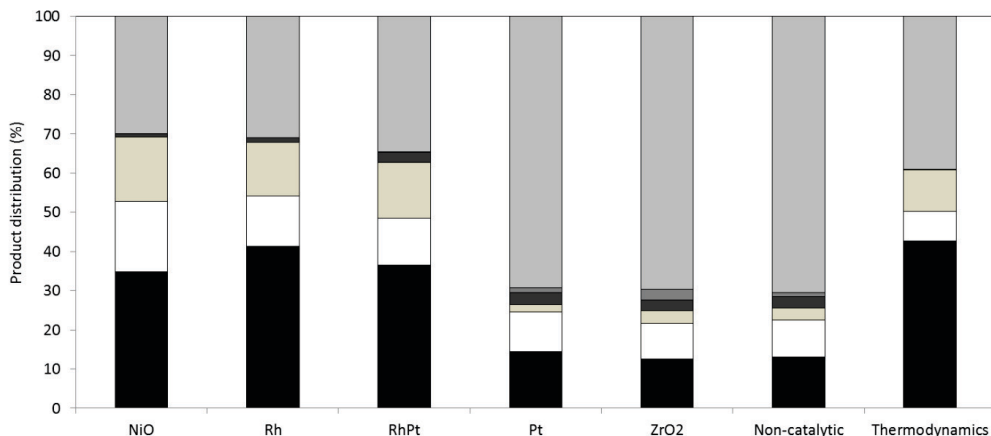


Figure 18. Average product distribution in ATR of ethanol at 700 °C, catalysts calcined at 700 °C (1 h). Hydrogen (■), carbon monoxide (□), carbon dioxide (■), methane (■), others (■), and water (■). (VI)

8.2.2 Effect of reforming temperature

Experiments at different temperatures demonstrated that complete conversion of ethanol is achieved on Rh-containing catalysts and the commercial catalyst at temperatures above 650 °C. With ZrO₂, with the Pt catalyst and in the thermal experiment complete conversion was achieved only above 800 °C. Although ZrO₂ had some activity in the ATR of ethanol, without the metallic sites it did not have sufficient reforming activity even at elevated temperatures. (VI)

According to the thermodynamics (VI), the production of methane reached a maximum at 200 °C and was negligible above 700 °C where MSR (Eq. 26) took place. The methane production followed the thermodynamics with the commercial NiO/Al₂O₃ and furthermore, it was lowest (1 mol-% at 700 °C) with this catalyst which was known to be highly active in MSR. With other catalysts the maximum methane production was detected at temperatures higher than predicted by the thermodynamics, varying from 700 °C for the Rh-containing catalysts to 800 °C for the monometallic Pt catalyst. The production of methane was highest with the noble metal catalysts (close to 11 mol-%).

Light HC (ethane, ethene, etc.) were detected in the product stream when the conversion of ethanol was incomplete, e.g., at low temperatures (<700 °C). Although thermal cracking reactions accelerated with temperature, the formation of light HC was negligible in the presence of the noble metal catalysts. (VI)

8.2.3 Stability of noble metal catalysts

The stability of the noble metal catalysts was studied at 700 °C for 24 h with the Rh, Pt, and RhPt catalysts. Slight deactivation of the Rh catalysts was detected towards the end of the test where the conversion of ethanol decreased to 95%. With the Pt catalyst, the conversion of ethanol remained stable at 64% over the whole stability test. Complete conversion of ethanol was, however, reached with the bimetallic RhPt catalyst for 24 h. The hydrogen production is presented in Figure 19. The hydrogen amount in the product mixture decreased over time with the monometallic catalysts, indicating some deactivation, while for the bimetallic catalysts the amount of hydrogen increased throughout the experiment indicating changes in the catalytic performance. (VI)

Because of the extensive formation of carbon deposits on NiO/Al₂O₃ under the reaction conditions the reaction had to be stopped after 20 min. However, the formation of carbon deposits after 5 h at 700 °C was strongest with the least active Pt catalyst (1.5 wt-%) and weakest with Rh (0.1 wt-%). With the bimetallic RhPt, the formation of carbon deposits accounted for 0.4 wt-%. Based on this, interaction between the two metals could be advantageous in terms of smaller formation of carbon deposits.

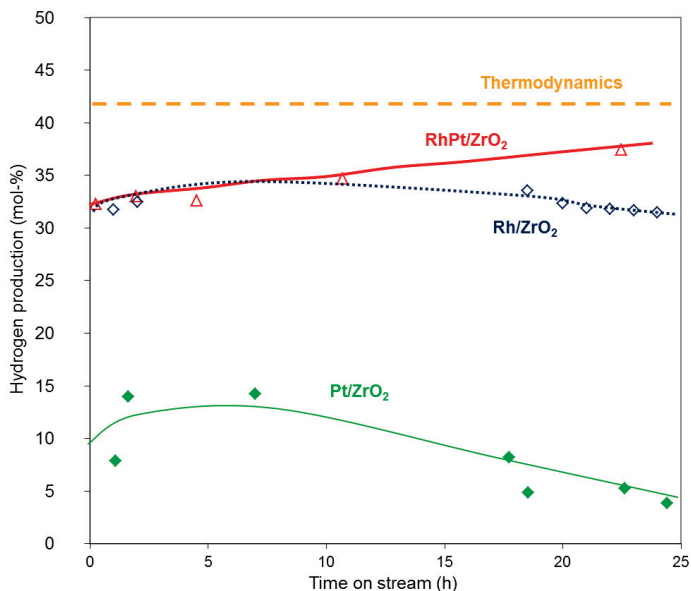


Figure 19. Hydrogen production achieved in the ATR of ethanol at 700 °C for 24 h. (VI)

The gasification reactions given in Eqs. 29-32 leading to the formation of hydrogen, methane, carbon monoxide, and carbon dioxide are possible under the experimental conditions tested. Also, noble metal and Ni catalysts were known to catalyze the methanation reaction (Eq. 27, [130]), increasing the production of methane. With the noble metal catalysts the maximum methane production was detected at temperatures higher than the one predicted by thermodynamics. Furthermore, the methane production was higher on the noble metal catalysts than on the commercial NiO/Al₂O₃ catalyst, the accumulation of carbon deposits also being less severe. This was in agreement with the observation that noble metal catalysts are active in the gasification of carbon deposits, thus removing the carbon deposits from the surface of the catalyst [118], yielding methane, carbon monoxide, hydrogen, and carbon dioxide (Eqs. 29-33) as products. Thus, most of the methane produced on the noble metal catalysts could be the result of the gasification of carbon deposits formed during the test. Methane production was lowest with the NiO/Al₂O₃ catalyst, but large amounts of carbon deposits were present after the experiment. This indicated a lower activity of the commercial NiO/Al₂O₃ catalysts for gasification reactions. It must be noted that this catalyst possessed high activity for methane reforming reactions, which might decrease the amount of methane. Because of the high amounts of methane produced on the noble metal catalysts, these catalysts might be more active for gasification reactions and less active in methane reforming than the NiO/Al₂O₃ catalyst. (VI)

8.3 Sulfur tolerance and autothermal reforming of commercial diesel

The effect of sulfur-containing feeds in ATR was tested using 4,6-DMDBT and hydrogen sulfide as model compounds. The results achieved with both sulfur-containing compounds are presented in Figure 20, where they are compared with the results achieved with a commercial low-sulfur diesel (< 10 ppm S). (IV)

The conversions and product distribution achieved with the addition of 4,6-DMDBT (as 10 ppm sulfur) were similar to those of commercial low-sulfur diesel. Slight deactivation of the bimetallic catalyst was detected as the conversions of D and T (simulated diesel, mixture of D and T) and water decreased and the production of hydrogen decreased with time. Furthermore, hydrogen sulfide was not detected in the product flow within the temperature range studied (400-900 °C). (IV)

The presence of 4,6-DMDBT brought about a slight decrease in the performance of the catalyst (Figure 20), but the amounts of all products decreased upon adding only 10 ppm of sulfur as hydrogen sulfide to the feed. After 6 h of experiment the hydrogen sulfide flow was stopped and the activity of the catalyst improved rapidly, but the product distribution and conversion achieved at 700 °C in sulfur-free conditions were not reached. However, the values corresponded to those obtained after 6 h in the presence of 4,6-DMDBT. Consequently, the deactivation caused by hydrogen sulfide was mainly reversible, but some irreversible deactivation also occurred at low temperatures [131]. (IV)

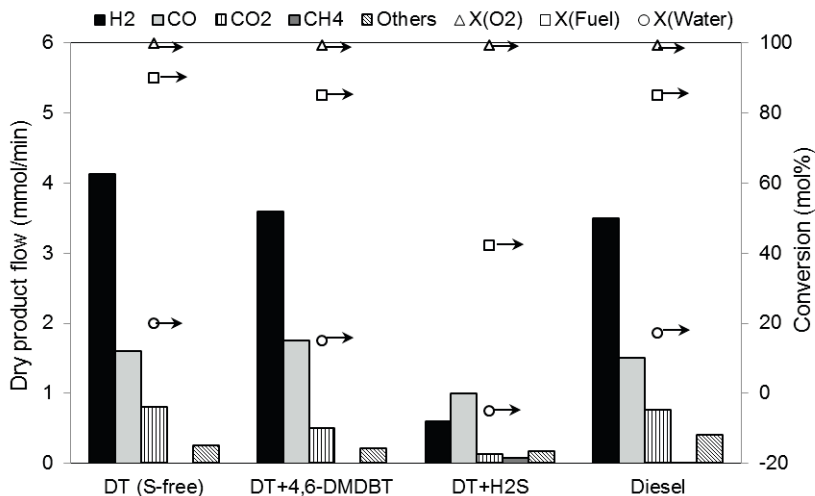


Figure 20. Effect of 4,6-DMDBT and hydrogen sulfide on the conversion (X_i) (oxygen Δ , fuel \square , water \circ) and dry product flows (mmol/min) in ATR of simulated (D= dodecane and T= toluene) and commercial (diesel) low-sulfur fuel on RhPt/ZrO₂ catalyst. Conditions: 700 °C, $H_2O/C= 3$, $O_2/C= 0.34$, sulfur (S) 10 ppm. (IV)

In the presence of hydrogen sulfide, the conversions of water and fuel decreased while the conversion of oxygen was not affected. Only the reforming activity of the catalyst was reduced, the oxidation activity remaining constant. This suggested that reforming and oxidation reactions took place on distinct active sites of the catalyst.

The deposition of carbon on the catalysts was least intensive in testes performed with hydrogen sulfide (IV) suggesting that the sulfur-containing compound adsorbed on the catalyst prevented the deposition of carbon either by blocking certain active sites of the catalyst or promoting carbon gasification reactions (Eqs. 29-33) [132,133]. The prevention of carbon monoxide adsorption has been reported for Ru- [133], Rh- [134], and Ni-based [132] catalysts in the presence of hydrogen sulfide. Also reforming has been reported to take place on a smaller ensemble of active sites than the adsorption of CO [86,132,134]. Hence, some sulfur on the catalyst minimized carbon deposition without interfering with the STR activity. The active sites for oxidation were not blocked by hydrogen sulfide as the conversion of oxygen remained complete.

9 Concluding remarks

New feedstocks for fuels are needed with the increasing demand for liquid fuels and the depletion of fossil fuels. While different options are available for electricity, e.g., solar, wind, hydropower, and hydrogen, for liquid fuels and chemicals biomass is the only alternative as a carbon source. Wood-based pyrolysis oil could be used as a source for liquid fuels and chemicals, although extensive catalytic treatment is needed to improve its physical and chemical properties.

Hydrogen and hydrogen-rich mixtures (synthesis gas) are promising energy sources as they are more efficient and cleaner than existing fuels, especially when they are used in fuel cells. In the long term, a hydrogen-based economy could provide energy security. Hydrogen can be produced from several feeds (e.g. biogas, biomass, biobased ethanol, gasoline, and diesel), for example, by using catalytic methods such as autothermal reforming.

Noble metal catalysts were active and selective in the hydrotreatment of guaiacol as model compound for the lignin fraction of wood-based pyrolysis oil and wood-based pyrolysis oil, and in the autothermal reforming of simulated gasoline and diesel, low-sulfur diesel, and ethanol. Although the systems studied were different, similarities in the behavior of the catalysts were observed. In hydrotreatment and autothermal reforming, rhodium-containing catalysts were the most active. Despite all the advantages of noble metal catalysts, their price is a drawback for industrial applications because of the large amounts required.

The results confirmed the interaction between the noble metals in the bimetallic catalysts. Adding platinum to the rhodium catalysts improved the stability of the catalyst. Furthermore, low calcination temperatures (400-700 °C) were desired in the preparation of the mono- and bimetallic catalysts as the encapsulation of the metal in the support was avoided and therefore, catalysts with higher activity were obtained.

Commercial catalysts are used in the sulfide form in hydrotreatment. When almost sulfur-free or completely sulfur-free feedstocks are hydrogenated, a sulfiding agent is added to the feed to keep the sulfided nickel-molybdenum and cobalt-molybdenum in

their active form. Without the addition of sulfur to the system, sulfur is lost from the active phase of the catalyst causing its deactivation. In the both cases, sulfur is detected in the products, meaning that the sulfur needs to be stripped out from the product, increasing the complexity of the processes.

Noble metal catalysts underwent reduction as activation procedure before hydrotreatment. Thus, there was no contamination of feedstocks or products with sulfur. No pretreatment was needed in autothermal reforming with noble metal catalysts. As shown in the autothermal reforming with low-sulfur diesel and hydrogen sulfide, noble metal catalysts tolerated some sulfur in the feed. Furthermore, as the conversion of hydrocarbons and water decreased and the conversion of oxygen was not affected by the presence of hydrogen sulfide in the feed, it could be concluded that only the reforming activity of the catalyst was reduced while the oxidation activity remained. This suggested that reforming and oxidation reaction take place on distinct active sites of the catalyst.

Noble metal catalysts were active in the hydrotreatment of guaiacol as a model compound for the lignin fraction of wood-based pyrolysis oil. The operation temperature had a significant impact on the product composition. At low temperatures (100 °C) mainly oxygen-containing hydrogenated compounds were obtained, whereas at high temperatures (300 °C) almost complete oxygen removal was achieved with less hydrogenated products. The use of lower temperatures reduced the occurrence of thermal cracking reactions. Carbon was lost to the gas phase in the form of carbon dioxide and methane (the main product in the gas phase), but low or no concentrations of carbon monoxide were detected.

Comparison of the results for guaiacol with the ones for the wood-based pyrolysis oil revealed that the correspondence was not straightforward. Although pyrolysis oil had guaiacol or similar groups that resulted from the thermal cracking of lignin, other compounds, e.g., sugars, were also present that behaved in a different way than guaiacol under the conditions tested. For this reason, adapting the data obtained with model compounds to systems involving real feedstock has to be done with caution.

The correspondence between the results achieved with model compounds and real feedstock was good in the autothermal reforming of diesel. Differences were detected when using hydrogen sulfide as a model compound for the sulfur-containing compounds of low-sulfur diesel. It was thus concluded that hydrogen sulfide was not a good model compound. Instead, 4,6-dimethyldibenzothiophene was more suitable as the results achieved with the simulated fuel and 4,6-dimethyldibenzothiophene and a commercial low sulfur diesel were similar.

Less carbon deposition was observed in hydrotreatment and autothermal reforming on noble metal catalysts than with commercial catalysts. Due to extensive formation of carbon deposits, the reforming of ethanol was not possible with commercial nickel catalyst in the used reactor system. However, using a rhodium on zirconia catalyst the experiments were successful.

The carbon dioxide thermograms from the temperature programmed oxidation measurements for noble metal catalysts used in the hydrotreatment of pyrolysis oil exhibited a broad peak with maximum at 360-370 °C only differing in intensity between catalysts. This suggested that the carbon deposited on the catalysts had a similar structure or that the nature and activity of the noble metal catalysts for the gasification of carbon species were similar.

The carbon deposits could be completely burnt in air as was shown in the Raman spectra: no differences were detected for the fresh and the regenerated catalyst. However, further testing is required to determine if there is a difference between the activity of the fresh and the regenerated catalysts. The low amounts of carbon deposited in the hydrotreatment of guaiacol and wood-based pyrolysis oil suggested that noble metal catalysts are more promising for large scale applications than commercial sulfided alumina-supported cobalt-molybdenum catalyst.

Traces of support material and metals were detected in the hydrotreated product achieved with the commercial alumina-supported cobalt-molybdenum catalyst in short batch tests. However, no leaching of metals (palladium, platinum, or rhodium) or support (zirconia) was detected in the hydrotreatment of pyrolysis oil. Although continuous tests are needed to confirm this, the noble metal catalysts tested seemed to be not only active but also stable under the harsh conditions of hydrotreatment.

Although the rhodium-containing noble metal catalysts exhibited good stability in autothermal reforming of model compounds and commercial low-sulfur diesel, further testing of these catalysts in the hydrotreatment of biomass-derived liquids in continuous reactors is required.

10 References

- [1] C. Fraiture, M. Giordano, Y. Liao, *Water Policy* 1 (2008) 67.
- [2] M.W. Rosegrant, T. Zhu, S. Masangi, T. Sulser, *Review of agricultural economics* 3 (2008) 495.
- [3] G.W. Huber, S. Iborra, A. Corma, *Chem. Rev.* 106 (2006) 4044.
- [4] Anon. www.ec.europa.eu/transport/themes/urban/cts/doc/2011-01-25-future-transport-fuels-report.pdf (13.01.2013).
- [5] A. Demirbas, *Prog. Energy Combust. Sci.* 33 (2007) 1.
- [6] D. Rutz, R. Janssen, *Biofuel Technology Handbook*, WIP Renewable Energies, Germany, 2007.
- [7] Anon. European Commission, *Hydrogen energy and fuel cells, A vision of our future*, Brussels, Belgium 2003. ISBN 92-894-5589-6.
- [8] P. Ferriera-Aparicio, M.J. Benito, J.L. Sanz, *Catal. Rev.-Sci. Eng.* 47 (2005) 491.
- [9] C. Song, *Catal. Today* 77 (2002) 17.
- [10] Anon. Commission of the European Communities, *An EU Strategy for Biofuels*, Brussels, Belgium 2006.
- [11] Anon. On the promotion of the use of energy from renewable sources, Directive 2009/28/EC of the European Parliament and of the Council, April 2009.
- [12] Anon. *Biofuels in the European Union, A vision for 2030 and beyond*, 2006.
- [13] Anon. www.forest.fi (24.11.2012).
- [14] Anon. Statistics Finland. 2009. *Energy Statistics Year Book 2008*, Official Statistics of Finland, Helsinki, Finland. ISBN 978-952-467-996-1.
- [15] Anon. Statistics Finland, www.statisticsfinland.fi (25.03.2013).
- [16] J. Väkevä, Finland's green gold, www.forestindustries.fi (25.11.2012).
- [17] A. Pirraglia, R. Gonzalez, D. Saloni, *Biomass Magazine*, www.biomassmagazine.com/articles/3853/wood-pellets-an-expanding-market-opportunity/ (12.01.2013).
- [18] A.V. Herzog, T.E. Lipman, D.M. Kammen, *Renewable Energy Sources in Encyclopedia of Life Support Systems (EOLSS) Forerunner Volume "Perspectives and Overview of Life Support Systems and Sustainable Development," Part 4C. Energy Resource Science and Technology Issues in Sustainable Development – Renewable Energy Sources*, www.eolss.com (12.01.2013).
- [19] E. Sjostrom, *Wood Chemistry: Fundamentals and Applications*, 2nd edition, Academic Press, San Diego, CA, US, 1993, p. 292.
- [20] D.L. Miller, *Biotechnol. Bioeng. Symp.* 5 (1975) 345.
- [21] X. Deglise, A. Donnot, A. Dufour, *Thermo-chemical conversion of recovered wood*, Presentation at COST E31 Management of Recovered Wood, 3rd and final Conference, Klagenfurt, Austria, May 2007.
- [22] Anon. www.bioenergy-noe.com/?_id=156 (11.01.2013).

- [23] Anon. www.journeytoforever.org/biofuel_library/WoodEthanolReport.html (27.11.2012).
- [24] Anon. Cellulosic Ethanol, Research Advances, National Renewable Energy Laboratory, Battelle, US, 2007, p. 1.
- [25] G.W. Huber, A. Corma, *Angew. Chem. Int.* 46 (2007) 7184.
- [26] S. Freni, S. Cavallaro, N. Mondello, L. Spadaro, F. Frusteri, *J. Power Sources* 108 (2002) 53.
- [27] Anon. www.iea.org/techno/essentials3.pdf (09.03.2013).
- [28] Anon. www.btgworld.com (11.01.2013).
- [29] A. Demirbaş, *Energy Convers. Manage.* 42 (2001) 1357.
- [30] A.V. Bridgwater, S. Czrnik, J. Piskorz, In *Fast Pyrolysis of Biomass: A Handbook*, Ed. A.V. Bridgwater, Antony Rowe LTD, Chippenham, UK, 2002, p. 1.
- [31] D. Mohan, C.U. Pittman, P. Steele, *Energy Fuels* 20 (2006) 848.
- [32] Anon. Wärtsilä Corporation, *Liquid Biofuel Power Plants*, Helsinki, Finland, 2013, p. 1.
- [33] S.R.A. Kersten, W.P.M. van Swaaij, L. Lefferts, K. Seshan, In *Catalysis for Renewables-From Feedstocks to Energy Production*, Eds. G. Centi, R.A. van Santen, Wiley-VCH, Weinheim, Germany, 2007, p. 119.
- [34] A. Oasmaa, E. Kuoppala, Y. Solantausta, *Energy Fuels* 17 (2003) 433.
- [35] J.H. Marsman, J. Wildschut, F. Mahfud, H.J. Heeres, *J. Chromatogr. A* 1150 (2007) 21.
- [36] A. Centeno, E. Laurent, B. Delmon, *J. Catal.* 154 (1995) 288.
- [37] F. Miguel de Mercader, M.J. Groeneveld, S.R.A Kersten, R.H. Venderbosch, J.A. Hogendoorn, *Fuel* 89 (2010) 2829.
- [38] A.V. Bridgwater, *Catal. Today* 29 (1996) 285.
- [39] R.K. Sharma, N.N. Bakhshi, *Can. J. Chem. Eng.* 69 (1991) 1071.
- [40] R. Maggi, B. Delmon, *Biomass Bioenergy* 7 (1994) 245.
- [41] A.V. Bridgwater and M.-L. Cottam, *Energy & Fuels* 6 (1992) 113.
- [42] A. Bridgwater, *Appl. Catal. A* 116 (1994) 5.
- [43] E. Furimsky, *Appl. Catal. A* 199 (2000) 147.
- [44] B. Donnis, R.G. Egeberg, P. Blom, K.G. Knudsen, *Top. Catal.* 52 (2009) 229.
- [45] O.I. Senol, T.-R. Viljava, A.O.I. Krause, *Catal. Today* 106 (2005) 186.
- [46] Anon. www.nesteoil.com, (09.03.2013).
- [47] Anon. www.uop.com/processing-solutions/biofuels/green-diesel/#natural-oils-conversion, (28.04.2013).
- [48] Anon. www.uop.com/processing-solutions/biofuels/green-jet-fuel/, (28.04.2013).
- [49] T.V. Choudhary, C.B. Phillips, *Appl. Catal. A* 397 (2011) 1.
- [50] E. Laurent, B. Delmon, *Appl. Catal. A* 109 (1994) 97.
- [51] G. de la Puente, A. Gil, J.J. Pis, P. Grange, *Langmuir* 15 (1999) 5800.
- [52] R.H. Venderbosch, A.R. Ardiyanti, J. Wildschut, A. Oasmaa, H.J. Heeres, *J. Chem. Technol. Biotechnol.* 85 (2010) 674.
- [53] J.I. Gray, L.F. Russell, *J. Am. Oil Chem. Soc.* 56 (1979) 36.

- [54] H. Topsøe, B.S. Clausen, F.E. Massoth, *Hydrotreating Catalysis – Science and Technology*, Eds. J.R. Anderson, M. Boudart, Springer – Verlag, Heidelberg, Germany, 1996, p. 310.
- [55] O.İ. Şenol, T.-R. Viljava, A.O.I. Krause, *Appl. Catal. A* 326 (2007) 236.
- [56] O.İ. Şenol, E.-M. Ryymin, T.-R. Viljava, A.O.I. Krause, *J. Mol. Catal. A: Chem.* 27 (2007) 107.
- [57] O.I. Şenol, T.-R. Viljava and A.O.I. Krause, *Catal. Today* 100 (2005) 331.
- [58] O.I. Şenol, E.-M. Ryymin, T.-R. Viljava, A.O.I. Krause, *J. Mol. Catal. A: Chem.* 268 (2007) 1.
- [59] E.-M. Ryymin, M. L. Honkela, T.-R. Viljava, A.O.I. Krause, *Appl. Catal. A* 358 (2009) 42.
- [60] A.A. Peterson, F. Vogel, R.P. Lachance, M. Fröling, M.J. Antal, Jr., J.W. Tester, *Energy Environ. Sci.*, 1 (2008) 32.
- [61] E. Furimsky, *Appl. Catal. A* 199 (2000) 147.
- [62] D.C. Elliot, G.G. Neuenschwander, T.R. Hart, J. Hu, A.E. Solana, C. Cao, In *Science in Thermal and Chemical Biomass Conversion*, Eds. A.V. Bridgwater, E.N. Hogan, CPL Scientific LTD, Newbury, UK, 2006, p. 1536.
- [63] E. Furimsky, F.E. Massoth, *Catal. Today* 52 (1999) 381.
- [64] E. Laurent, B. Delmon, *J. Catal.* 146 (1994) 281.
- [65] V.N. Bui, D. Laurenti, P. Afanasiev, C. Geantet, *Appl. Catal. B* 101 (2011) 239.
- [66] B.M. Reddy, A. Khan, *Catal. Rev.* 47 (2005) 257.
- [67] G. Henriksson, J. Li, L. Zhang, M.E. Lindström, In *Thermochemical Conversion of Biomass to Liquids Fuels and Chemicals*, Ed. M. Crocker, RSC Publishing, Cambridge, UK, 2010, p. 222.
- [68] E. Sjöström, *Wood Chemistry – Fundamentals and Applications*, Academic Press, New York, US, 1981, p.223.
- [69] Anon. <http://www.chempattec-auhorn.com/stockprep/index.html>, 06.09.2013.
- [70] J. Mikulec, A. Kleinová, J. Cvangros, L. Joriková, M. Banic, *Int. J. Chem Eng.*, doi:10.1155/2012/215258.
- [71] E.L. Back, L.H. Allen, Eds., *Pitch Control, Wood Resin and Deresination*, TAPPI Press, Atlanta, GA, US, 2000.
- [72] R. Coll, S. Udas, W.A. Jacoby, *Energy & Fuels* 5 (2001) 2266.
- [73] J. Myllyoja, J. Aalto, E. Harlin, WO 2007003708 (A1) 2007.
- [74] I. Kubičková, D. Kubička, *Waste and Biomass Valorization* 1 (2010) 293.
- [75] P. Knuuttila, *Fuel* 104 (2013) 101.
- [76] P. Ferriera-Aparicio, M.J. Benito, J.L. Sanz, *Catal. Rev.-Sci. Eng.* 47 (2005) 491.
- [77] C. Song, *Catal. Today* 77 (2002) 17.
- [78] J. Rostrup-Nielsen, *Catal. Today* 63 (2000) 159.
- [79] S. Clarke, A. Dicks, K. Pointon, T. Smith, A. Swann, *Catal. Today* 38 (1997) 411.
- [80] Anon. *Hydrogen & Our Energy Future*, Hydrogen Program, US Department of Energy, www.hydrogen.energy.gov, (13.01.2013).
- [81] M. Ni, D.Y.C. Leung, M.K.H. Leung, *Int. J. Hydrogen Energy* 32 (2007) 3238.
- [82] M. Krumpelt, T.R. Krause, J.D. Carter J.P. Kopasz, S. Ahmed, *Catal. Today* 77 (2002) 3.
- [83] F. Joensen, J.R. Rostrup-Nielsen, *J. Power Sources* 105 (2002) 195.
- [84] S.H. Clarke, A.L. Dicks, K. Pointon, T.A. Smith, A. Swann, *Catal. Today* 38 (1997) 411.

- [85] S. Irusta, L. Cornaglia, E. Lombardo, *J. Catal.* 210 (2002) 263.
- [86] D.L. Trimm, *Catal. Today* 37 (1997) 233.
- [87] L. Wang, K. Murata, M. Inaba, *Ind. Eng. Chem. Res.* 43 (2004) 3228.
- [88] B. Li, K. Maruyama, M. Nurunnabi, K. Kunimori, K. Tomishige, *Appl. Catal. A* 275 (2004) 157.
- [89] T. Bruno, A. Beretta, G. Groppi, *Catal. Today* 99 (2005) 89.
- [90] Anon. www.noble.matthey.com, (30.04.2013).
- [91] M. Votsmeier, T. Kreuzer, G. Lepperhoff, Automobile exhaust control, In *Handbook of Fuels-Energy Sources for Transportation*, Ed. B. Elvers, Wiley-VCH, Weinheim, Germany, 2008, p. 299.
- [92] Anon. www.kd-chem.com/app-5.html, (10.10.2010).
- [93] T. Miyake, T. Makino, S.-I. Taniguchi, H. Watanuki, T. Niki, S. Shimizu, Y. Kojima, M. Sano, *Appl. Catal. A* 364 (2009) 108.
- [94] A. Tungler, T. Tarnai, L. Hegedű, K. Fodor, T. Máthé, *Platinum Met. Rev.* 42 (1998) 108.
- [95] A. Benedetti, G. Fagherazzi, F. Pinna, G. Rampazzo, M. Selva, G. Strukul, *Catal. Lett.* 10 (1991) 215.
- [96] L. Cornaglia, J. Múnera, E. Lombardo, *Appl. Catal. A* 263 (2004) 91.
- [97] S. Irusta, L. Cornaglia, E. Lombardo, *Mater. Chem. Phys.* 86 (2004) 440.
- [98] M.N. Barroso, M.F. Gomez, L.A. Arrúa, M.C. Abello, *Appl. Catal. A* 304 (2006) 116.
- [99] T. Yamaguchi, *Catal. Today* 20 (1994) 199.
- [100] M.H. Youn, J.G. Seo, I.K. Song, *Int. J. Hydrogen Energy* 35 (2010) 3490.
- [101] H. Yasuda, N. Masubayashi, T. Sato, Y. Yoshimura, *Catal. Lett.* 54 (1998) 23.
- [102] T. Mizuno, Y. Matsumura, T. Nakajima, S. Mishima, *Int. J. Hydrogen Energy* 28 (2003) 1393.
- [103] T. Yamaguchi, *Catal. Today* 20 (1994) 199.
- [104] R. Burch, P.K. Loader, *Appl. Catal. A* 143 (1996) 317.
- [105] S. Clarke, A. Dicks, K. Pointon, T. Smith, A. Swann, *Catal. Today* 38 (1997) 411.
- [106] U. Hennings, R. Reimert, *Appl. Catal. B* 70 (2007) 498.
- [107] T. Yamaguchi, *Catal. Today* 20 (1994) 199.
- [108] K. Tanabe, T. Yamaguchi, *Catal. Today* 20 (1994) 185.
- [109] N. Srisirawat, S. Therdthianwong, A. Therdthianwong, *Int. J. Hydrogen Energy* 34 (2009) 2224.
- [110] H. Idriss, *Platinum Met. Rev.* 48 (2004) 105.
- [111] J. Haber, B. Delmon, *Pure Appl. Chem.* 67 (1995) 1257.
- [112] J. Lehto, A. Oasmaa, Y. Solantausta, M. Kytö, D. Chiamonti, Fuel oil quality and combustion of fast pyrolysis bio-oils, *VTT Technology* 87, Espoo, Finland, 2013, pp. 79.
- [113] A. Roine, *HSC Chemistry for Windows 5.11* Outokumpu Research Oy (2003).
- [114] D.W. van Krevelen, *Fuel* 29 (1950) 269.
- [115] J.A. Moulijn, M. Makkee, A. van Diepen, *Chemical Process Technology*, Wiley, Weinheim, England, 2001, pp. 18.
- [116] H. Jiang, H. Yang, R. Hawkins, Z. Ring, *Catal. Today* 125 (2007) 282.
- [117] S. Derrouiche, D. Bianchi, *Langmuir* 20 (2004) 4489.

- [118] E.I. Kauppi, R.K. Kaila, J.A. Linnekoski, A.O.I. Krause, M.K. Veringa Niemelä. *Int. J. Hydrogen Energy* 35 (2010) 7759.
- [119] M.M. Hossain, *Chem. Eng. J.*, 123 (2006) 15.
- [120] D.C. Elliott, G.F. Schiefelbein, *Preprints of Papers – American Chemical Society, Division of Fuel and Chemistry* 34 (1989) 1160.
- [121] D.C. Elliott, A. Oasmaa, *Energy Fuels*, 5 (1991) 102.
- [122] M. Guisnet, P. Magnoux, *Appl. Catal. A* 212 (2001) 83.
- [123] S.K. Bej, S.K. Maity, U.T. Turaga, *Energy Fuels* 18 (2004) 1227.
- [124] X. Rozanska, R. van Santen, F. Hutschka, J. Hafner, *J. Catal.* 205 (2002) 388.
- [125] A. Suopanki, R. Polvinen, M. Valden, M. Härkönen, *Catal. Today* 100 (2005) 327.
- [126] M.M.V.M. Souza, M. Schmal, *Catal. Lett.* 91 (2003) 11.
- [127] J.H. Bitter, K. Seshan, J.A. Lercher, *J. Catal.* 176 (1998) 93.
- [128] D.K. Liguras, D.I. Kondarides, X.E. Verykios, *Appl. Catal. B: Environ.* 43 (2003) 345.
- [129] A.C. Basagiannis, P. Panagiotopoulou, X.E. Verykios, *Top. Catal.* 51 (2008) 2
- [130] D. Kunzru, *Chemical Engineering Transaction* 13 (2008) 359.
- [131] C. Palm, P. Cremer, R. Peters, D. Stolten, *J. Power Sources* 106 (2002) 231.
- [132] J.R. Rostrup-Nielsen, *J. Catal.* 85 (1984) 31.
- [133] T. Suzuki, H.-I. Iwanami, T. Yoshinari, *Int. Hydrogen Energy* 25 (2000) 119.
- [134] J.J. Strohm, J. Zheng, C. Song, *J. Catal.*, 238 (2006) 309.



ISBN 978-952-60-5322-6
ISBN 978-952-60-5323-3 (pdf)
ISSN-L 1799-4934
ISSN 1799-4934
ISSN 1799-4942 (pdf)

Aalto University
School of Chemical Technology
Department of Biotechnology and Chemical Technology
www.aalto.fi

**BUSINESS +
ECONOMY**

**ART +
DESIGN +
ARCHITECTURE**

**SCIENCE +
TECHNOLOGY**

CROSSOVER

**DOCTORAL
DISSERTATIONS**